Review Article

Huibin Liu, Qinghao Guo, Wenhao Wang, Tao Yu, Zheng Yuan, Zhixing Ge, and Wenguang Yang*

A review of magnetically driven swimming microrobots: Material selection, structure design, control method, and applications

https://doi.org/10.1515/rams-2023-0119
received March 21, 2023; accepted September 04, 2023

Abstract: Magnetically driven swimming microrobot is a typical one in the family of microrobots and they can achieve navigation and manipulation in low Reynolds number biomedical environments with an external magnetic drive strategy. This study reviews recent advances in material selection, structure design, fabrication techniques, drive control method, and applications for magnetically driven swimming microrobots. First, the materials used in magnetically driven swimming microrobots were introduced and the effect of material selection on performance was discussed. Second, structure design of swimming microrobots and manufacturing techniques are reviewed, followed by a discussion on the main advances in effective motion control, path planning, and path tracking. Then, the multi-applications of magnetically driven swimming microrobots including targeted drug delivery, cell manipulation, and minimally invasive surgery are summarized. Finally, the current challenges and future directions of the work on magnetically driven swimming microrobots are discussed.

Keywords: magnetic microrobots, structure design, materials selection, manufacturing techniques

1 Introduction

In recent years, microrobots have also received focused attention from research scholars due to their tiny size and high maneuverability in new biomedical fields including targeted drug delivery and minimally invasive surgery [1–3]. Unlike most robots, microrobots require proprietary actuation strategies. Commonly used actuation strategies are physical actuation (light, magnetism, heat, electricity, ultrasound), chemical actuation (reagent reaction), and biological actuation (pollen, red blood cells, spirulina) [4]. Each driving strategy has made significant progress in research, but also has its own shortcomings. For example, electric actuation is promising for fuel-free motion, but electrodes limit the working area of the robot and biomedical applications [5,6]. Light actuation is simple and direct, but when the light intensity is too weak, it cannot penetrate the blocking tissues and affects the actuation of the microrobot. When the light intensity is too strong, the heat generated may damage biological materials and human tissues [7–9]. Considering the temperature sensitivity and limited self-regulation of human tissues and organs, thermal actuation may cause permanent damage to living tissues and organs [10]. Ultrasonic actuation is biocompatible, but its actuation mechanism and physical properties result in an inability to precisely control the direction of motion. Also, there are difficulties in operating in some tissues containing air bubbles [11–13]. Chemical reaction drives, while offering high maneuverability performance, mostly require the use of toxic fuels such as H_2O_2, N_2H_4, HCl, urea, and $NaBH_4$ [14,15]. In addition, the inability to control the reaction in real time once it has started and the very limited amount of fuel available for the reaction limit the operating time of the microrobot. These reasons have led to poor biocompatibility and operational stability of chemically driven microrobots [16,17]. Biological drives offer the advantages of a more complete structure, greater compatibility, faster response time, and the ability to be retrofitted for flexible movement. However, how to ensure the safety of the operation during biological manipulation and at the same time ensure the normal activity of living cells or microorganisms remain an important challenge for biologically driven technologies [18–20].

Magnetic actuators are able to penetrate tissue for precise non-contact manipulation. Moreover, it has been

* **Corresponding author: Wenguang Yang**, School of Electromechanical and Automotive Engineering, Yantai University, Yantai 264005, China, e-mail: ytu_yangwg@163.com
Huibin Liu, **Qinghao Guo**, **Wenhao Wang**, **Tao Yu**, **Zheng Yuan:** School of Electromechanical and Automotive Engineering, Yantai University, Yantai 264005, China
Zhixing Ge: State Key Laboratory of Robotics, Shenyang Institute of Automation, Chinese Academy of Sciences, Shenyang 110016, China

Open Access. © 2023 the author(s), published by De Gruyter. This work is licensed under the Creative Commons Attribution 4.0 International License.

proved by medical experiments that the method is harmless and without pollution to the human body under the magnetic field of low intensity [2]. In addition, in conjunction with clinically available equipment, magnetically actuated microrobots can be driven and manipulated by magnetic resonance imaging (MRI) systems, further increasing the potential for clinical applications. Compared to other drive methods, magnetic drive solves most of the problems and compensates for many shortcomings, and is now widely used in microrobots [21]. As shown in Figure 1a, the popularity of research on magnetically driven microrobot continues to rise [22].

Richard Feynman introduced the concept of microrobots in his 1959 keynote speech "There's Plenty of Room at the Bottom" at the annual meeting of the American Physical Society at Caltech. Since then, a systematic study of microrobot was initiated. In 1966, the film "Fantastic Voyage" imagined and showed the development of microrobots in the form of science fiction, and expressed the expectation of the research results of microrobots. In a paper entitled "Life in Low Reynolds Number" published in 1977, the authors discussed the fluid dynamics at low Reynolds numbers and summarized the scallop theorem on how to achieve effective motion. It points the way for the design and research of microrobots. In 2009, the first micrometer scale artificial bacterial flagellum (ABF) magnetically driven microrobot was successfully fabricated. Remote and flexible manipulation was achieved by providing uniform magnetic field drive control through a three-dimensional Helmholtz coil, which strongly confirms the feasibility of magnetically driven microrobots. Through further research on material properties, optimization of body structure, exploration of micro and nanofabrication technologies, and development of better control strategies, magnetically driven microrobots have become progressively more powerful and have improved their operational capabilities in the biomedical field. In particular, the movie "Big Hero 6" in 2014 made a science fictional vision of the

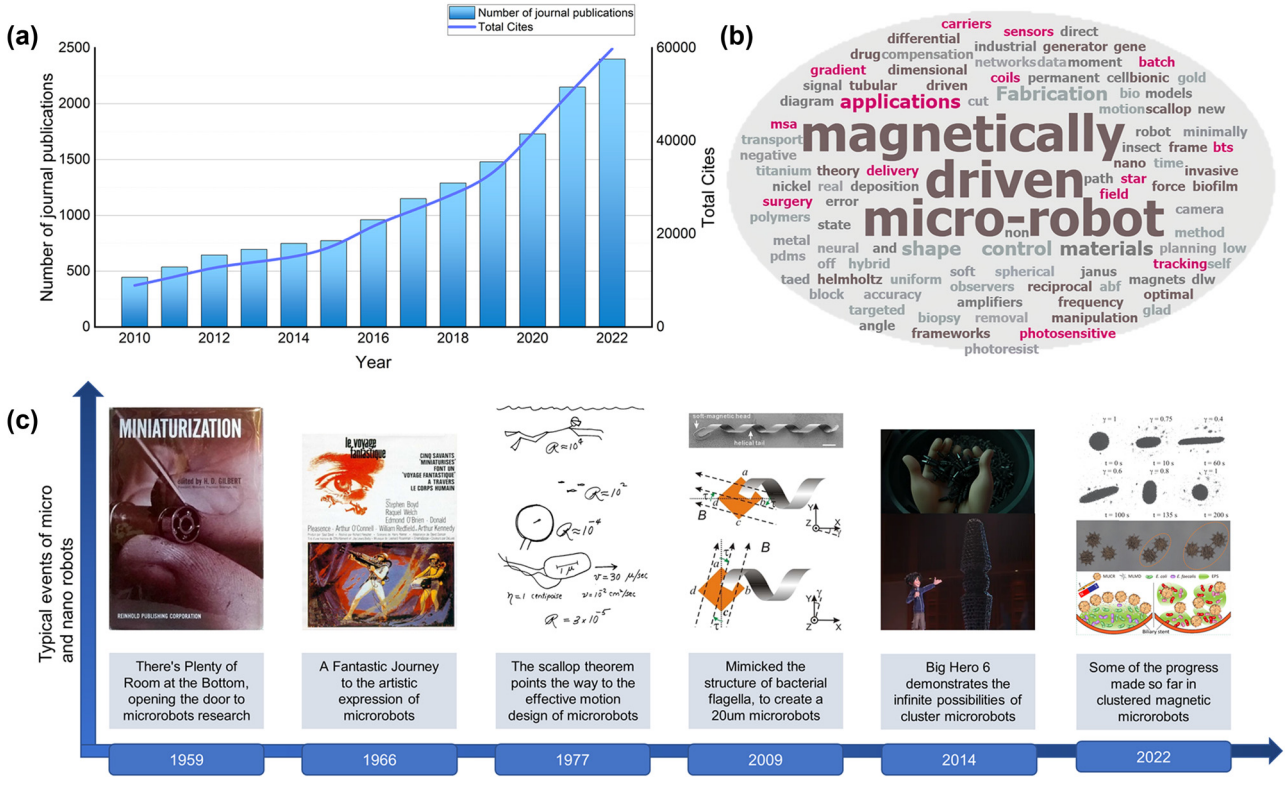

Figure 1: (a) The graph shows the number of journal publications and citations for magnetically driven microrobots 2010–2022. The data of journal publications were obtained from Google Scholar Jan 2023; the data of article citations were obtained from Web of Science Jan 2023. (b) Magnetically driven microrobot keyword word cloud. (c) Typical events in the development history of magnetically driven swimming microrobots. In 1959, the concept of microrobots was introduced in a lecture at the annual meeting of the American Physical Society at the California Institute of Technology, entitled, There's Plenty of Room at the Bottom. Imagining microrobots in the 1966 Fantastic Voyage film. The discussion of effective motion in the microscopic world in 1997 pointed to the direction of microrobot research and design; the successful experiment of manufacturing and controlling ABF microrobots in 2009. The Imagining of magnetically driven microrobot clustering capabilities by Big Hero 6 film. In 2022, some progress has been made in magnetically driven microrobot cluster technology.

clustering capability of magnetically driven microrobots, highlighting the power of their clustering capability in contrast to the limited nature of individuals, and also providing some inspiration for the subsequent development of magnetically driven microrobot clustering technology. In 2022, after constant exploration and research, scientists have made some progress in magnetically driven microrobot clustering technology. The results are in line with expectations, greatly enhancing the operational capability and efficiency of magnetically driven microrobots, and once again validating the great research potential of magnetically driven microrobots (Figure 1c).

Magnetically driven microrobots are often designed to operate in low Reynolds number microfluidic environments, where viscous forces are the primary resistance. So magnetically driven microrobots must break the reciprocity of motion to achieve net displacement [23,24]. Based on the scallop theory and combined with inspiration from the movement of microorganisms, the researcher has designed magnetic microrobots with structures such as helical and biohybrids to achieve effective movement. Responding to the manipulation of the driving magnetic field, Fe_3O_4 or NdFeB particles are distributed in an orderly manner on the body of the microrobots to achieve controlled non-reciprocating motion. In addition, to be suitable for special operations and fulfill the intended function, structures such as tubular, star, link worm, and bullet shapes are also designed [11,25–28]. Due to the programmability of the magnetic field [29], it can be combined with control algorithms such as proportional-integral-derivative (PID) control, sliding mode control (SMC), and so on. It can be designed as a complex control system for functional design and combined operation (*i.e.*, cluster control) of magnetically driven microrobots. Further, it can be combined with an optimal bidirectional RRT* path planning algorithm to fit the desired trajectory. Moreover, in order to improve the operational efficiency of microrobots, clustered magnetic-driven microrobots and cluster control technology are currently being developed. For example, microgear [30] and colloid [31] for realizing reversible motion and inverse gravity, swarm control strategy [31], and fuzzy adaptive regulation strategy [32], and so on. Greater progress has been made, greatly improving operational efficiency. In addition to effective structure and control system design, materials and fabrication are also important elements in the research application of magnetically driven microrobots. On the one hand, traditional manufacturing techniques are no longer applicable to the preparation of magnetic microrobots because of the difference in scale between magnetic microrobots and macroprocesses products [33]. Therefore, there is a need to explore new micro- and nanofabrication techniques, which are currently commonly used, such as direct lithography (direct laser writing; DLW), glancing angle deposition (GLAD), biotemplates (BTS), and template assisted electrochemical deposition (TAED). These fabrication techniques are capable of preparing complex structures at the micron level, realizing an important step towards the reality of microrobots. On the other hand, it is important to use different materials that meet the performance requirements as well as match the manufacturing technology. Most importantly, it is also important to ensure its safety [34]. Gradually, scientists have explored and developed materials such as using red blood cells as carriers, or using metal–organic frameworks (MOF) designed with Ni/Ti. Good biophilicity and workability were achieved in *in vitro* simulation tests. Combining these steps, the designed magnetically driven microrobot can be utilized for biomedical applications such as targeted drug delivery, cell manipulation and minimally invasive surgery. Not only does it provide a novel biomedical tool, but it promises great achievements in clinical medicine. Therefore, the study of magnetically driven microrobots integrates the exploration of material properties and micro and nanofabrication techniques, the design of structures and control systems, and its wonderfully diverse applications to form a whole that echoes each other (Figure 1b).

In this article, we comprehensively summarize the various components of magnetically driven microrobot research. As shown in Figure 2, first, the material properties and additional functions for the preparation of magnetically driven microrobots are presented. Then, various structural designs of magnetically driven microrobots and their characteristics are listed. Next an overview of the latest developments in micro- and nanofabrication technologies that enable magnetically driven microrobot preparation is presented. On this basis, the control system design of the magnetically driven microrobot is summarized. Then, a series of applications of magnetically driven microrobots are presented. Finally, the current challenges and future directions of magnetically driven microrobots are analyzed.

2 Material selections for magnetically driven swimming microrobots

Different materials used for magnetically driven swimming microrobots can affect their mobility (kinematic performance, and maneuverability) and functional properties

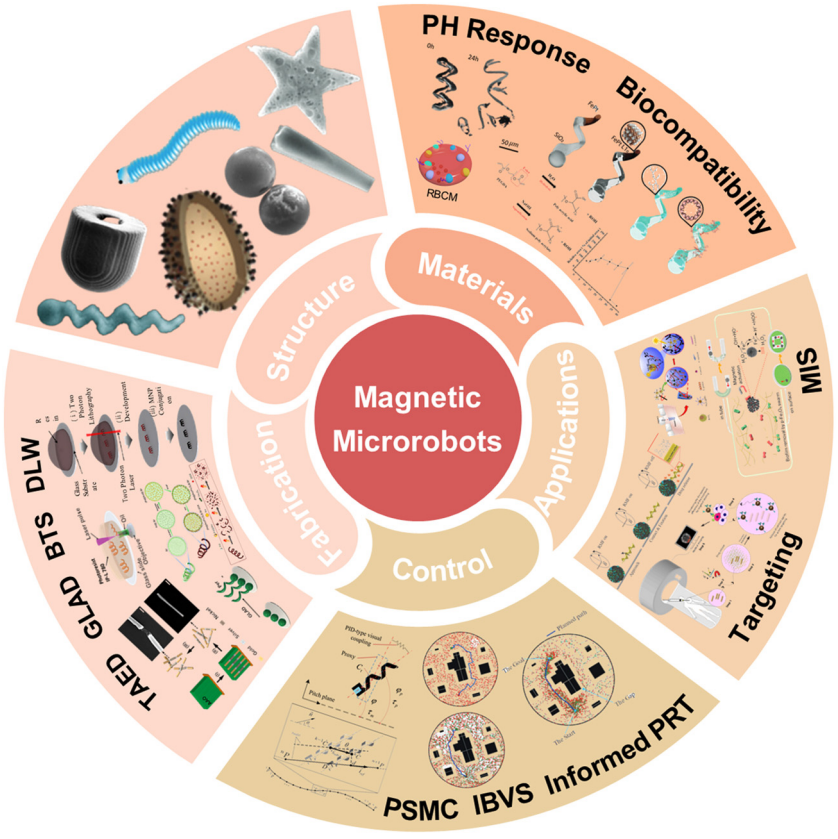

Figure 2: This study reviewed the materials, structure design, fabrication techniques, navigation control, and applications of magnetically driven swimming microrobots.

(degradability, hydrophobicity, and biophilicity). Therefore, the study of material properties of magnetic microrobots is of great significance for the development of magnetic microrobots. Based on the results of the effects on magnetic microrobots, their materials can be divided into magnetic and functional materials, corresponding to the mobility and functional properties, respectively.

2.1 Magnetic materials

The magnetic material is primarily used to drive manipulation in response to an external magnetic field [35]. According to the difficulty of magnetization of magnetic materials magnetization rate (xm), magnetic materials can be classified as ferromagnets (xm >> 0), paramagnets (xm > 0), and antimagnate (xm < 0) [36]. Paramagnets and antimagnate have a weak attraction or repulsion to the magnetic field, and once the magnetic field is removed, the magnets cannot retain any magnetization. Ferromagnets exhibit very high magnetism when subjected to a magnetic field, and are able to retain a certain level of magnetism even after the magnetic field is removed [37]. High remanent magnetism is a characteristic of hard ferromagnets, also known as permanent magnets, when subjected to a magnetic field. In contrast to the performance of hard magnetic materials, soft magnetic materials exhibit low remanence after being subjected to the same magnetic field [38]. Both hard and soft magnets exhibit some hysteresis behavior, and when demagnetizing these materials, an opposing coercive magnetic field is necessary. Correspondingly, the more remanent magnetism there is, the higher the coercivity. Therefore, hard magnets have high coercivity and soft magnets have low coercivity. Superparamagnetic magnets are a class of special materials with high magnetization, no remanence, and no coercivity [39].

Although there are some microrobots that are driven by paramagnetic material response, such as reported by Yu *et al.* who utilized dynamic magnetic field controlled disassembly of paramagnetic nanoparticles to efficiently transport cargo into confined areas [40]. However, as shown in Table 1, most small size robots are composed of ferromagnets and superparamagnetic compounds. Ferromagnetic materials such as Ni, Fe, and NdFeB are widely used not only for their high saturation magnetization strength but also for their ability to perform microrobot drives and flexible manipulation at low magnetic field strengths.

Table 1: Materials, manufacturing methods, applications, properties, and structural references of some typical structures of magnetically driven swimming microrobots

Structure design	Synthetic materials	Fabrication methods	Microrobot features	Applications	Speed ($\mu m \cdot s^{-1}$)	Size (μm)	Ref.
Helical structured	Photosensitive polymers, Ni, Au	DLW	Surface coating hydrophobicity affects motion characteristics	Targeted drug delivery	62.5	15 × 5	[52]
	Zinc-based MOF, ZIF-8, Ni	DLW	MOF- based; biocompatibility and pH responsive	Targeted drug delivery	50	10	[45]
	PEGDA700, MNPs, ethylenediamine	Two-photon lithography (TPL)	Magnetic nanoparticle retrieval ability	Targeted drug delivery	160	100 × 35	[70]
	SiO_2, Ni, perfluorocarbon silane	GLAD	Magnetic microrobots penetrate biological tissue for operation	Minimally invasive surgery	0.7–11.4	5×10^{-2}	[33]
	Fe, Pt, SiO_2	GLAD	Biocompatible helical magnetic microrobots for fabrication and cell transfection	Cell manipulation	24	1.5	[113]
	PEGDA, PETA, Fe_3O_4	TPP	Active controlled drug release and thermal therapy treatment, degradable	Minimally invasive surgery	82	120	[48]
	Ormocomp, PMMA, PDMS, Ti, Fe	DLW	Helical structure noninvasive zygote transfer	Cell manipulation	≈800	130–170	[137]
Biohybrid structured	RBCs, IGG, Fe_3O_4	BTS	RBCM, active cancer phototherapy	Targeted drug delivery	56.5	≈2	[49]
	Pine pollen, Fe_3O_4	BTS	Pollen cavities for drug and magnetic particle loading transport	Targeted drug delivery	175.19	25	[50]
	Unicellular green microalgae, magnetic polystyrene	BTS	Helical magnetic microalgae with structural integrity and biocompatibility	Targeted drug delivery	≈109.54	20	[47]
	S. platensis, $BaTiO_3$, Fe_3O_4	BTS	Magneto piezoelectric, single cell navigation operation	Cell manipulation	333.3	≈22 × 0.6	[86]
	Spirulina platensis, Fe_3O_4	BTS	Photosynthesis improves medical conditions and radiotherapy results	Minimally invasive surgery	21.7–78.3	≈50	[87]
JM	Ni, Pt	Electron beam evaporation (EBE)	Highly maneuverable multimodal microrobot	Cell manipulation	50–200	10–50	[34]
	NPs, Au, GDYO, BP, Pt, MnO_2, Fe_2O_3	EBE	Multimodal high performance microrobots	Targeted drug delivery	18–142	17	[94]
	Ni, Au, SiO_2	SD	Similar to the rolling and crawling motion of leukocytes in the wall of the tube	Targeted drug delivery	600	3–7.8	[46]
Bullet structured	Resin, Ni, propylene glycol	TPP	Magnetic field assisted control of compound drives	Minimally invasive surgery	2,250	90	[11]
Annular structure	PDMS, Ni, Fe	GLAD	Bionic type effective motion microrobot	Targeted drug delivery	≈100	≈40–100	[26]
Star structured	PVA, ALG, Fe_3O_4	TAED	Specially structured effective motion design at low Reynolds number, degradable	Targeted drug delivery	4–17	4 × 40	[27]

Note: PEGDA, poly(ethylene glycol) diacrylate; MNPs, magnetic nanoparticles; PETA, pentaerythritol triacrylate; PMMA, Poly methyl methacrylate; PDMS, poly(dimethylsiloxane); RBCs, red blood cells; IGG, indocyanine green; Ormocomp, a negative tone photoresist; PM, commercially available superparamagnetic microspheres; GDYO, Graphdiyne oxide; PVA, polyvinyl alcohol; ALG, antilymphocyte globulin.

The higher the saturation magnetization strength, the greater the magnetic force in the field and the better the maneuverability. In the kinematic design of a magnetically driven microrobot, ferromagnets are distributed according to a specified position and then follow a programmed magnetic field for a specific motion. For example, Jang *et al.* used Ni as a magnetic coating to achieve flexible motion manipulation on a magnetically driven fluctuating microrobot integrated by several rigid sections [41]. In addition, NdFeB, as a representative of hard magnetic materials, has excellent remanent magnetization characteristics and at the same time is able to provide more power. For example, Li *et al.* doped porous silica spheres into NdFeB-silicon-elastomer substrates to prepare strongly stable multimodal magnetic microrobots [42]. This microrobot shows effective response to operational impediments in a work environment with multiple interferences. Darmawan *et al.* developed a pH responsive magnetic microrobot by embedding a pH responsive layer and NdFeB magnetic nanoparticles (MNPs) in a composite resin [43]. Not only is it biocompatible, but it is also able to be imaged by X-rays and is expected to be used in the treatment of gastric cancer. Gu *et al.* developed a self-folding soft robotic chain with reconfigurable shape and function using NdFeB magnets and flexible hinges [44]. Not only is it compatible with current magnetic navigation technology, but it offers many desirable features and functions that are difficult to achieve through existing surgical tools.

In addition to their rich functionality, microrobots with ferromagnets have great maneuverability. When considering its kinematic performance, the ratio of kinematic speed to microrobot (C) is greater than 1, and most of them can be greater than 5. The prime example is a microrobot with a MOF designed using Ni/Tiv [45], and a magnetic Janus microrobot fabricated using Ni/Pt alloy [34]. Some are even greater than 10 [33,46], and their speed of movement is several times their body length, which fully illustrates their excellent athletic performance.

However, due to the toxicity of Ni to cells [47], it does not meet biomedical requirements. Therefore, Fe, FePt, NdFeB, and Fe_3O_4 magnetic particles and other iron compounds are gradually becoming the magnetic materials commonly used in microrobots at present. It avoids or mitigates cytotoxicity as much as possible based on good magnetic response characteristics. Meanwhile, it can be combined with novel materials such as biological templates (red blood cells and pollen) or polymers (poly(ethylene glycol) diacrylate; PEGDA) to create structurally integrated magnetic microrobots with enhanced operational capabilities [27,48–50].

2.2 Material characteristics requirements

To meet the requirements for its applications in biomedicine, magnetic microrobots also requires functional properties such as degradation, enhanced surface hydrophobicity, and low or no toxicity by selecting the corresponding functional materials. In addition, the magnetic microrobot body has to be prepared in a way that is compatible with the material requirements of the fabrication technology in order to achieve the target preparation.

2.2.1 Degradability

Biodegradability is an important factor in the operation of microrobots *in vivo*, which not only reduces the recycling efforts of microrobots, but also avoids accidental microrobot residues. Dong *et al.* prepared helical soft microrobots with magnetoelectric (ME) properties by two photon lithography using light cured gelatin methacrylamide (GelMA). As magnetic microrobot-mediated electromagnetic stimulators of neuronal cells, soft microcones prepared by GelMA are degraded by enzymes secreted by the cells [51]. Optical images show the degradation process of ME helical soft cone shaped microrobots after 0, 1, 3, and 7 days (Figure 3a). Zn-based MOFs zeolite imidazole framework-8 (ZIF-8) coated magnetic helical microrobot with biocompatible and pH responsive properties was prepared by Wang *et al.* ZIF-8@ABFs showed significant biodegradation after being placed in an acidic solution at pH 6 for 12 h (Figure 3b). Besides, cancer cells often survived in an acid environment, which makes the ideal materials for drug delivery applications in cancer therapy [45]. Park *et al.* designed a magnetically driven swimming microrobot made of PEGDA and pentaerythritol triacrylate (PETA), where the ester group was hydrolyzed to polyacrylic acid and an alcohol fraction (PEG or polyelectrolyte; PE) as a byproduct (Figure 3c).

These microrobots are controlled to degrade and realize the purpose of the operation while ensuring the safety of the *in vivo* operation [48]. In addition, by choosing different materials, these microrobots have a variety of different properties to meet the needs of different operating environments and some of the necessary conditions for future translation into clinical applications.

2.2.2 Hydrophilicity and hydrophobicity of surface

In addition to degradability, the hydrophilicity and hydrophobicity of surface are another important factor in the

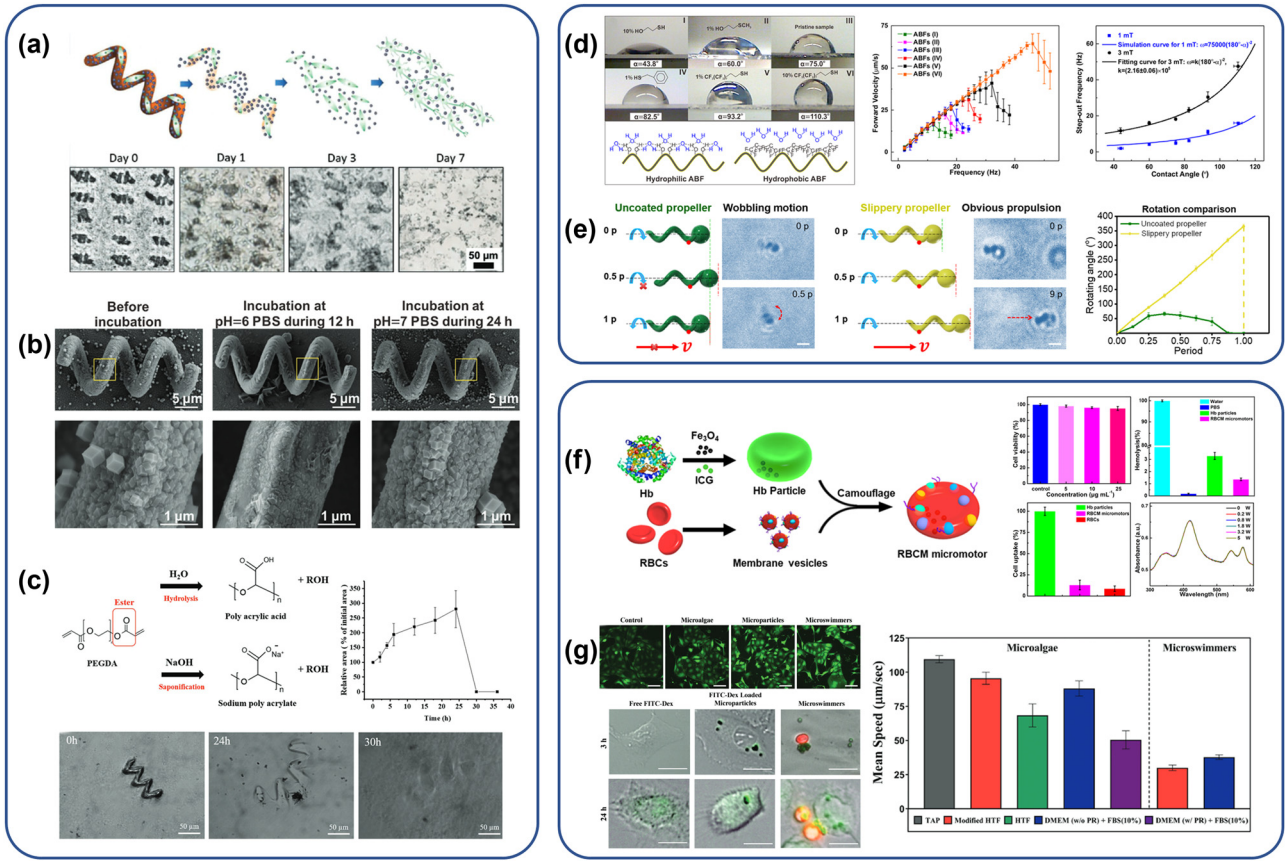

Figure 3: Material properties of magnetically driven swimming microrobots. (a) Optical images of the degradation process of soft magnetic microrobots with cells after 0, 1, 3, and 7 days of incubation, respectively. Reproduced from Ref. [51] with permission from Advanced Functional Materials. (b) SEM images of the degradation process of microrobots based on MOF. Reproduced from Ref. [45] with permission from Advanced Materials. (c) Time lapse diagram of the degradation process of magnetic microrobots made of PEGDA and PETA. Reproduced from Ref. [48] with permission from Advanced Healthcare Materials. (d) Modification of the surface chemistry of magnetic microrobots, thus changing the overall hydrophobicity. Reproduced from Ref. [52] with permission from ACS Nano. (e) Surface functionalization of microrobots by vapor deposition of perfluorosilane and fusion with a smooth perfluorocarbon liquid layer to change the lubricity of the microrobot surface. Reproduced from Ref. [33] with permission from Science Advances. (f) Structural characterization of simulated erythrocyte microrobots, and characterization of bioaffinity capabilities. Reproduced from Ref. [49] with permission from ACS Applied Materials & Interfaces. (g) Comparative experiments on algal microrobots in cell culture and characterization of biocompatibility of such materials. Reproduced from Ref. [47] with permission from Advanced Materials.

study of microrobot materials. By modifying the hydrophilicity of the magnetic microrobot surface, it is possible to enhance its lubricity or adhesion in the operating environment. Thus, it is easier to traverse narrow tissue gaps or adhere steadily to the work area, facilitating the completion of the work task. Wang *et al.* controlled the hydrophobicity by modifying the surface chemicals of magnetically driven swimming microrobots to transport targeted drugs. The experiments confirmed that microrobots with hydrophobic surfaces exhibited larger cutoff frequencies and higher maximum forward velocities than those with hydrophilic surfaces (Figure 3d) [52]. Wu *et al.* investigated a helical magnetically driven swimming microrobot at the 2 μm level to penetrate a biological barrier. In order to effectively reduce the adhesion of the microrobot to the biopolymeric network, the microrobot was surface functionalized by vapor deposition of perfluorosilane and fusion with a smooth perfluorocarbon liquid layer to enhance the surface lubricity (Figure 3e) [33]. Wang *et al.* attached a biopolymer film made of chitosan-glycerol (C-G) solution to the surface of a magnetic microrobot, and prepared a toroidal magnetic soft robot that utilized mucosal adhesion motion [53]. By controlling the concentration of glycerol and the mucosal adhesion time, the contact area and the adhesive force of the mucous membrane can be regulated, resulting in strong motility on surfaces with different geometries and orientations.

Surface functionalization of magnetically driven microrobots not only improves the kinematic performance, but also matches the operating environment inside the human

body, which is more conducive for the execution of operational tasks. In addition, compared to the development of new materials, it greatly reduces the difficulty of research and improves the feasibility of design.

2.2.3 Biocompatibility

The biocompatibility of the microrobot is another important consideration in the development of the magnetically driven swimming microrobot. With good biocompatibility, microrobots can reduce accidental interference and carry out operational tasks more smoothly. Gao *et al.* designed an acoustically driven and magnetically navigated red blood cell mimicking microrobot (RBCM) by modifying the red blood cell structure. The cytotoxicity and working capacity of the RBCM microrobot was examined and analyzed by controlled experiments in cell culture. The results indicate that RBCM has good cytocompatibility and resistance to phagocytosis (Figure 3f) [49]. Yasa *et al.* designed a biohybrid microrobot composed of a Chlamydomonas reinhardtii, which can be navigated by a magnetic field from a natural species. Microalgal robots meet good biocompatibility to be studied for medical applications. It was concluded from experiments that the algal hybrid microrobots remained highly active in blood solutions and showed good biocompatibility with both healthy and cancer cells (Figure 3g) [47]. Moreover, Li *et al.* also demonstrated that magnetic biohybrid microrobots based on diatoms have high drug loading capacity and pH sensitivity in addition to good biocompatibility [54]. In addition, Ye *et al.* developed a folic acid targeted magnetic microrobotic system using a hydrogel network of GelMA and a magnetic MOF with a porous structure [55]. The composite magnetic microrobot is characterized by good biocompatibility, long *in vivo* circulation time, high magnetic response sensitivity, and stable nature.

Good biocompatibility allows magnetic microrobots to have longer *in vivo* operation time, and more stable functional structure. In addition, immune rejection in the human body is largely avoided, ensuring the stability of magnetic microrobot operations.

3 Structure design of magnetically driven swimming microrobots

3.1 Helical

Researchers designed a helical magnetic microrobot consisting of a spiral structured tail and a magnetic head body by studying the flagellar structure and its role in microorganisms such as bacteria [56]. By applying a magnetic torque to the helical microrobot under a low intensity rotating magnetic field, the rotation can be converted into linear motion and achieve effective motion in a low Reynolds number environment due to the structure of the helix [57,58]. And by switching the external magnetic field, the reverse motion of the spiral robot can be easily achieved [59]. The researchers found that propulsion performance of helical microrobot treated with surface hydrophobicity is better [45,60].

Bacterial flagellated magnetically driven swimming microrobots are often referred to as ABF [61]. The first implementation of drive control for a helical structured magnetically driven swimming microrobot was developed by Zhang *et al.* in 2009. The magnetic material with a length of 15.7 μm and a diameter of 4.3 μm was coated by electron beam evaporation, as shown in Figure 4a. Precise propulsion and steering could be controlled by uniformly strong rotating magnetic field drive [61]. To improve functionality, Xu *et al.* developed spiral magnetically driven swimming microrobots for transporting sperm (Figure 4b). Cylindrical slotted holes were used to replace the original lamellae, and the surface was coated with Fe and TiO_2 films to improve magnetic response and biocompatibility. Magnetic microrobots integrated with synthetic protein-based hyaluronic acid (HA) microchips bound to the sperm HA receptor by interaction. After transportation to the designated location, the microchip is degraded by a localized protease enzyme, allowing the spermatozoa to escape and successfully achieving the sperm transportation task [62]. To further improve the biocompatibility, Ceylan *et al.* designed a microrobot based on enzymatically degraded hydrogel, which consists of GelMA and superparamagnetic iron oxide particles. Microrobots can completely degrade responding to pathological concentrations of matrix metalloproteinase-2 (MMP-2), thereby facilitating the release of embedded cargo molecules (Figure 4c) [63]. Considering the complexity of the *in vivo* environment, Huang *et al.* designed a reconfigurable structure of the helical microrobot [64]. As shown in Figure 4d, after receiving external stimulation, the structure of the microrobot is transformed from the initial folded state to a morphology with complementary helix angles, which realizes the modal transition of the microrobot with multimode control. Moreover, this modal transformation is reversible and can be effectively used for targeted drug delivery at complex sites through complex tissue structures such as narrow pores. Zheng *et al.* used a single step anisotropic plating method to fabricate modules with different functions, which were then composed into a modular microrobot (MMR) [65]. Cells and MNPs, drugs, and contrast

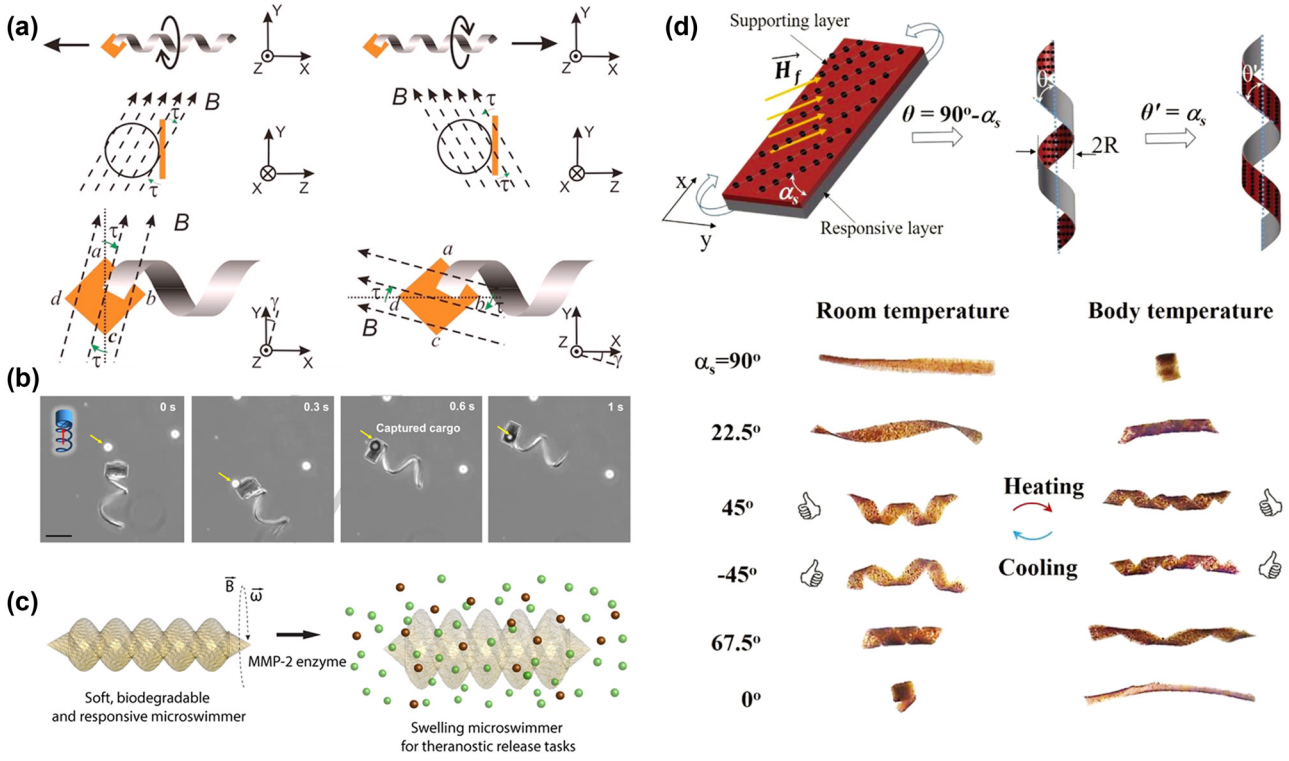

Figure 4: Design of a typical helical magnetically driven swimming microrobot. (a) Motion control of a helical microrobot under a rotating magnetic field. Reproduced from Ref. [61] with permission from Applied Physics Letters. (b) Time shift diagram of a microrobot consisting of a cylindrical slotted hole and a helical tail, moving under a drive control field. Reproduced from Ref. [62] with permission from Chem. Int. Ed. Engl. (c) Microrobots rapidly respond to pathological concentrations of MMP-2 through lysis, thereby facilitating the release of embedded cargo molecules. Reproduced from Ref. [63] with permission from Acs Nano. (d) Structure transformation triggered by external stimuli (heat) transforms the initial folded structure into a refolded structure with complementary helix angles. Reproduced from Ref. [64] with permission from Adv. Funct. Mater.

agents were loaded onto different hydrogel microstructured modules of MMR. By programming the electric field, the microscale strips can be endowed with a variety of shape deformations, such as spirals, twists, bends, and coils. Driven and manipulated by a magnetic field, the MMR can achieve two movement modes, fishlike and caterpillar-like, in an environment that simulates human blood vessels. In addition, to facilitate the manipulation of modular magnetic microrobots, Sokolich *et al.* developed a low-cost, portable and multifunctional manipulation device (ModMag) [66]. The device is equipped with several electromagnetic configurations such as three-dimensional Helmholtz, two-dimensional four-coil, and two-dimensional magnetic tweezers, expanding the usage scenarios of magnetically driven microrobots. In addition, to avoid the side effects of damage to the organism caused by residual MNPs, extensive study is conducted for providing effective solution [48,51,67–70]. For instance, Lee *et al.* developed a helical magnetic microrobot capable of hydrolysis for effective recovery of MNPs in the organism using dithiothreitol (DTT) reducers and near infrared (NIR) external stimulation [70]. In general, due to the precise and controlled motion characteristics of the helical magnetically driven swimming microrobots, great progress has been made in biomedical research, environmental pollution removal, *etc.* The next research will focus on the *in vivo* tracking and cluster control of the helical magnetically driven swimming microrobots to improve the feasibility and efficiency of *in vivo* operations.

3.2 Biohybrid

Biohybrid microrobots rely on a combination of magnetic particles with biological microorganisms (*e.g.*, plant and animal cells and bacterial magnetic particles) [47,49,50,71]. The hybrid microrobots have attracted the attention of researchers due to their complete system structure, good biocompatibility, deformability, and low or no toxicity [72–74]. Currently, the design of magnetic biohybrid microrobots is mainly based on the adaptive modification of cells and microalgae.

Recently, a large number of cell-based swimming microrobots have been developed for use in biomedical research [75]. Among them, erythrocytes are often used as biohybrid microrobot carriers due to their long cycle time (100–120 days), and large manipulable space volume [76,77]. Gao *et al.* developed a red blood cell mimetic microrobots (RBCMs) driven by an acoustic field with magnetic field manipulation to control the direction of motion (Figure 5a) [49]. In their study, magnetic hemoglobin nuclide encapsulated photosensitizers (PSs) were wrapped with natural red blood cell membranes to prepare RBCMs for photo dynamic surgery by actively transporting oxygen. In addition, Nguyen *et al.* successfully encapsulated an anticancer drug within the attached liposomes of macrophages. Under the control of an external magnetic field drive, this biohybrid microrobot move to targeted cancer cells at an average speed of 10.47 ± 4.46 $\mu m \cdot s^{-1}$. Then, targeted drug delivery was achieved to kill cancer cells [78]. Sperm cells can provide a degree of protection against degradation of drug by immune response [79–81]. Therefore, sperm cells are also widely used in magnetically driven biohybrid microrobots. Magdanz *et al.* combined deactivated sperm cells with magnetic microparticles by electrostatic interaction, to prepare magnetic biohybrid microrobots called IRONSperms [82]. And the experimental results show that in the rotating magnetic field constructed by electromagnets, IRONSperms can achieve effective propulsion in the low Reynolds number due to its helical flagellar structure, and thereby enabling targeted drug delivery. In addition to animal cells, some plant cells have the potential to be transformed into biohybrid microrobots. Pollen cells have a spatially voluminous pollen cavity that can be used to carry targeted drugs, and they also have good structural homogeneity and biocompatibility [83,84]. Zhang *et al.* directly deposited magnetic particles on naturally porous spores followed by encapsulation with functionalized micro carbon particles to remotely detect toxins secreted by *Clostridium difficile* [85].

Furthermore, scientists have discovered that some microalgae (*e.g.*, *Spirulina platensis*, *Spirulina obtusifolia*) have excellent properties for efficient spiral propulsion.

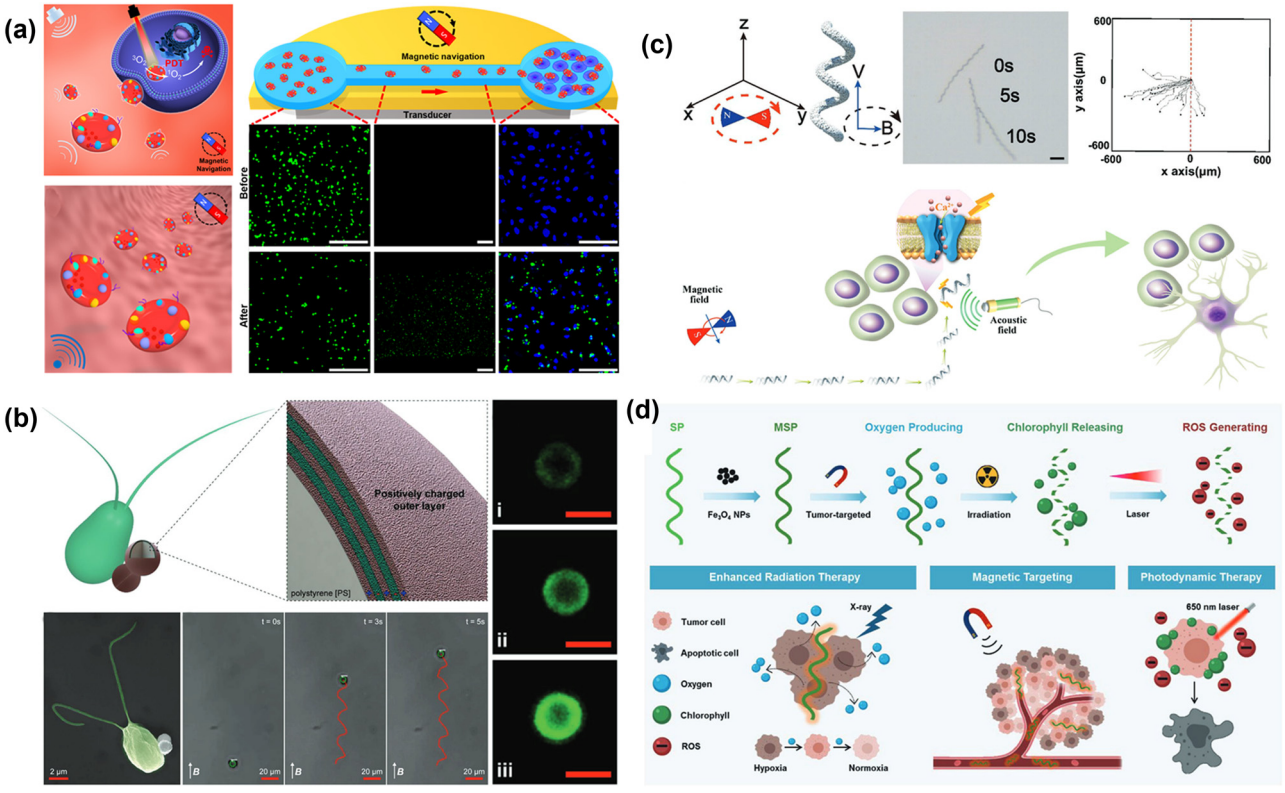

Figure 5: Functional characterization of biohybrid microrobots. (a) Conceptual diagram of an acoustic field driven, magnetic field guided erythrocyte simulation microrobot, and experimental demonstration of design effectiveness. Reproduced from Ref. [49] with permission from ACS Appl. Mater. Interfaces. (b) Noncovalent electrostatic interaction between positively functionalized magnetic polystyrene (PS) particles and negatively charged microorganisms is used to noninvasively attach the carrier to the microalgae without affecting their natural movement. Reproduced from Ref. [47] with permission from Adv. Mater. (c) Microrobots for precise electrical stimulation of neuronal cells to induce differentiation of target neural stem cells. Reproduced from Ref. [86] with permission from Advanced Functional Materials. (d) Photosynthetic biohybrid nanoswimmers act as oxygen generators to regulate the tumor microenvironment through *in situ* oxygen generation by photosynthesis in hypoxic solid tumors. Reproduced from Ref. [87] with permission from Adv. Funct. Mater.

Yasa *et al.* prepared a magnetic microalgae robot for cargo delivery by attaching microalgae (*C. reinhardtii*) to a PE surface treated with functionalized MPs particles [47] (Figure 5b). Non-invasive transportation of goods without affecting magnetic microrobot motions is achieved by utilizing nonmetric electrostatic interactions between magnetic PS particles and microorganisms. Liu *et al.* developed *S. platensis*@Fe_3O_4@t-$BaTiO_3$ microrobots using spirulina (*S. platensis*) as a biological template. Utilizing the highly controllable nature of magnetic microrobotics, electrical signals can be precisely delivered to achieve directional movement of cells to induce differentiation of target neural stem cells (Figure 5c) [86]. Meanwhile, this study expands the application of magnetically actuated microrobots, which show good potential for neuronal therapy. Zhong *et al.* designed a biohybrid magnetic microrobot that can generate O_2 based on the modification of *Spirulina platensis* (*S. platensis*). They used Fe_3O_4 NPs as O_2 generators to improve the effectiveness of radiotherapy by modulating the tumor cell environment (Figure 5d) [87]. In addition, several research groups based on Spirulina have developed magnetic biohybrid microrobots that hold potential for targeted drug delivery/therapy [88,89].

Plant and animal cells, as well as microalgae, naturally have a complete and complex structure. After being modified and treated, it becomes a good magnetic microrobot carrier for *in vivo* cargo transportation. Compared to organoid structures prepared using proprietary materials by micro- and nanofabrication techniques, biohybrid carriers are not only more readily available, but also more stable overall. In addition, biohybrid structures typically have better performance, as well as properties such as biocompatibility, and are also more suitable for operations in complex environments within the body. Magnetic biohybrid microrobots possess a more complete structure. Finally, biohybrid structures enable a closer crossover between micro and nanotechnology and biotechnology, providing new ideas and approaches in biomedical and biomanufacturing fields.

3.3 Spherical

Spherical magnetic microrobots usually consist of Janus particles. It contains drive parts that respond to external magnetic fields, and functional parts for targeted drug delivery transport [90]. Due to their simple structure and functional integration, they are favored by researchers. There is a large amount of research in biomedical applications, and environmental remediation [91].

Spherical magnetic microrobots are mostly designed based on the functional properties of their constituent Janus particles. According to the driving characteristics of Janus particles, the spherical magnetic microrobots can be classified into single, hybrid, and cluster types. The spherical microrobot composed of magnetically sensitive Janus particles is a typical design for a single drive, having the ability to perform two different functions simultaneously, magnetic field remote manipulation and accurate orientation [92]. Inspired by the locomotor behavior of leukocytes in the circulatory system, Alapan *et al.* designed a multifunctional microroller (Figure 6a). Microrollers, composed of Janus particles, half respond to external magnetic field drive and half to biochemical functional processing. Through cell specific antibodies and drug molecules on the microrollers, it achieves targeted delivery of therapeutic drugs [46]. Feng *et al.* designed a novel anticancer drug delivery system with Fe_3O_4 NPs for target localization, rhodamine B for fluorescent tracing, and paclitaxel for killing cancer cells [93]. This method could reduce overdose administration and avoidance of associated side effects. Based on a single drive, in order to enhance the operational capability of the spherical microrobot, the hybrid drive design is proposed. Wang *et al.* developed a multimodal spherical microrobot based on magnetic hollow Janus microspheres (JM). Magnetically sensitive layers respond to external magnetic fields to control orientation, and microbubble rupture to generate jets to provide the driving power (Figure 6b). In addition, using the hydrodynamic effect of microbubble rupture, we can effectively regulate the motion performance of spherical microrobots [34]. Yuan *et al.* used Janus particles wrapped in nanomaterials to develop bubble-optical-magnetic multiengine spherical microrobot (Figure 6c). The driving units can be combined under certain conditions to achieve adaptive drive control of spherical microrobots [94]. Based on the development of single and hybrid drives, and in order to further improve the working capability of spherical microrobots, cluster (cooperative) control design is proposed. Li *et al.* designed a dimeric microrobot consisting of two magnetic JMs. Under external oscillating magnetic fields, the microspheres rolled alternately like “feet” to traverse the complex environment with precision and flexibility [95]. In addition, Yu *et al.* designed a trimeric microrobot composed of magnetic Janus colloids. Under an external rotating magnetic field, it has multimodal locomotion and selective reconfigurable capabilities [96]. Jin *et al.* used paramagnetic and conductive magnetite NPs as building blocks to guide groups of microrobots to form ribbons under a programmed magnetic field. Moreover, the structure can be reversibly expanded to connect disconnected electrodes to construct electron conduction pathways (Figure 6d). Further, an attempt was made to mimic the behavior of ant clusters and construct unconventional cluster structures [97].

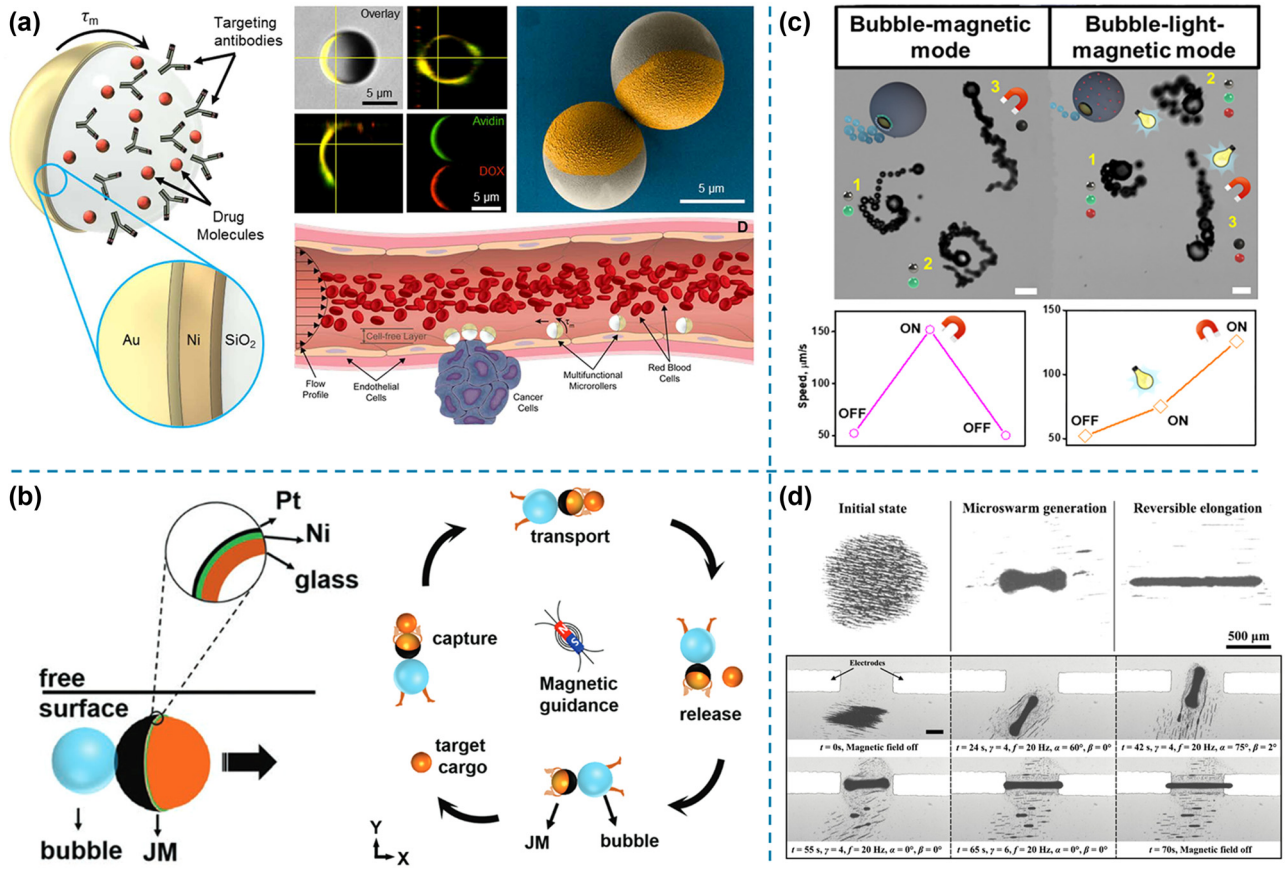

Figure 6: Janus spherical microrobot functional features. (a) A spherical microrobot composed of spherical Janus particles, one half with magnetic response to magnetic field drive, one half with biochemical and loading capabilities of silica, and a conceptual diagram of flow in a blood vessel. Reproduced from Ref. [46] with permission from Sci. Robot. (b) Multimodal and highly mobile bubble microrobot, powered by a jet generated by the bursting of microbubbles, with a magnetically sensitive layer embedded in the JM surface responding to external magnetic field modulation, enabling remote control of the spherical microrobot. This figure is reproduced from Ref. [34] with permission from Small. (c) Bubble magnetic, bubble light magnetic, modular, multiple engine spherical microrobot schematic. Reproduced from Ref. [94] with permission from Chemistry of Materials. (d) Programmed oscillating magnetic fields, the building blocks are reconfigured as ribbon microclusters, simulating the structure and function of ant bridges in a microcluster system. Reproduced from Ref. [97] with permission from ACS Nano.

Through research and development in recent years, spherical magnetic microrobots have made remarkable achievements in terms of functionality and operability. Whereas existing research has shown that cluster (cooperative) control of spherical microrobots can significantly improve maneuverability, future research will also focus on this direction.

3.4 Other structures

In order to be better suited to certain operational situations, the researchers have also developed other structures of magnetic microrobots while meeting the basic requirements. Examples include tubular, linked worms, stars, bullets, soft body microrobots, flagellums, guidewires, rigid junctions, and multipedal structures.

Tubular magnetic microrobots are not only simple to build but also offer great advantages in single cell capture, transport, and release [98]. Yang *et al.* achieved simple fabrication of 3D microtubes by setting up structured optical vortices in magnetic photoresist. By further adjusting the phase factor of the optical vortex, 3D microtubules can also be fabricated into chiral structures (Figure 7a). After the surface is coated with Fe_3O_4 magnetic layer, it is precisely manipulated by external magnetic field. For cell manipulation and other biomedical research, it provides an effective manipulation tool [25]. The microrobot with annelid structure is driven by magnetically controlled preload and has good motion performance. Liu *et al.* prepared tubular ZIF-8 magnetic microrobots by using the unique

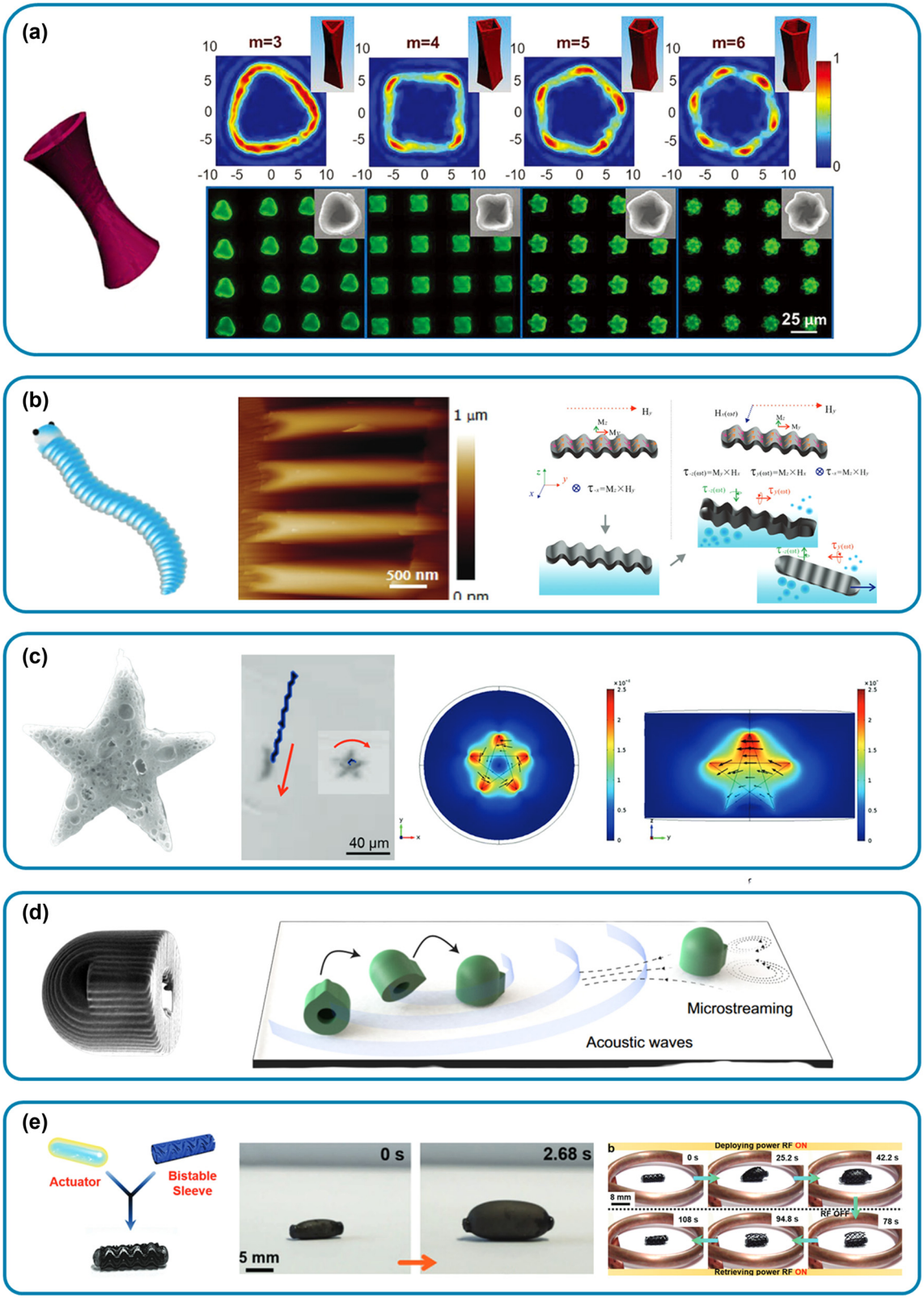

Figure 7: Schematic diagrams of tubular, annelid, star, bullet, and hose microrobots. (a) Modulation of 3D microtubule geometry. Reproduced from Ref. [25] with permission from Advanced Functional Materials. (b) Structural and kinematic characteristics of annelid microrobots, representative atomic force microscopy (AFM) images of ordered fold patterns. This figure is reproduced from Ref. [26] with permission from Small. (c) Time lapse images of spin and roll motion of magnetically driven stellar hydrogel microrobots. Reproduced from Ref. [27] with permission from Macromolecular Chemistry and Physics. (d) Schematic diagram of US driven, magnetically guided microrobot motion. Reproduced from Ref. [11] with permission from Proceedings of the National Academy of Sciences. (e) Proof of concept schematic for reversible bistable magnetron stent application. Reproduced from Ref. [28] with permission from Advanced Materials.

hollow structure of kapok fibers and combining bubble actuation and external magnetic control [99]. Based on the mixed correlation effect, the dense ZIF-8 layer can effectively adsorb organic pollutants on microrobots, showing great potential for wastewater treatment. Liu *et al.* inspired by the structure of a ringworm prepared magnetic microrobots with a ringworm structure by applying pre-stress on the substrate. Its peak velocity in an oscillating magnetic field is approximately 100 $\mu m \cdot s^{-1}$, and it has excellent hydrodynamic properties even in the complex environment of flow. And because of its large surface area, it also has good "cargo" transport capabilities (Figure 7b) [26]. Hu *et al.* used hydrogel polymers to prepare a magnetic microrobot with a star shaped structure. Under the external rotating magnetic field, vertical rotation (rolling) is done, and by interacting with the substrate, they achieve flexible manipulation (Figure 7c). Moreover, based on the biocompatibility of hydrogels, the immune response caused by external foreign body microrobots is greatly mitigated [27]. Aghakhani *et al.* developed a bullet-shaped magnetic microrobot with hybrid acoustic-magnetic drive. Using acoustic resonance to excite the bubble to provide power, the magnetically sensitive site responds to an external magnetic field to control the direction (Figure 7d). While maintaining good power, it also ensures control accuracy and is suitable for narrow space exploration [11]. Bhalla *et al.*, through improved design of this structured microrobot, further improved its mobility performance and control accuracy [90]. To solve the problem of weak power and poor working ability of micro soft robots, Tang *et al.* designed a magnetic phase change soft microrobot, by combining the thermally responsive polymeric soft body robot with a magnetic scaffold, which was prepared as a bistable and reversible composite device (Figure 7e). Moreover, the performance of the composite device is approximately 106 times higher than the performance of conventional soft body microrobots. It greatly improves the ability of soft body microrobots for applications such as medical and artificial muscles [28].

In addition, due to the representativeness of the flagellar structure in the microscopic realm, scientists have expanded their research on it. For example, Striggow *et al.* studied the beat pattern of the sperm cell flagellum and summarized the relationship between changes in beat pattern and movement. In turn, a new magnetic sperm microrobot beat pattern is proposed to improve its overall performance in complex biofluids. The designed magnetic sperm microrobot was experimentally demonstrated to be able to move efficiently in bovine oviductal fluid and viscoelastic medium [80]. To minimize the trauma that guidewires and catheters can cause to the body during current vascular procedures, Yang *et al.* developed an ultrasound (US)-guided manipulable magnetic guidewire. By establishing a mathematical model between the applied magnetic field and the deformation of the end of the guidewire, the attitude of the guidewire can be effectively estimated, and thus the procedure can be performed more precisely. Furthermore, the use of such a magnetic guidewire system avoids the radiation safety issues associated with fluoroscopic imaging [100]. In addition, Zhang *et al.* have further expanded the materials and functionality of the magnetically guided filament to develop a mass-producible and 3D manipulable magnetically guided filament. This magnetically guided wire is made using commercially available wires, connected to a soft driver made of Ecoflex coupled magnetic powder. In addition, the device has a large workspace of 700 mm × 500 mm × 500 mm and is capable of a wide range of deflection angles, resulting in a wider range of applications and uses [101]. Zong *et al.* summarized the efficient locomotion strategy of fluctuating propulsion by summarizing the microbial locomotion modes, and developed a magnetic microrobot consisting of a spring connected to four rigid parts [102]. The structure enables agile and controllable fluctuating motion under an external oscillating magnetic field. Liao *et al.* further investigated magnetic microrobots with rigidly connected structures, using 3D laser lithography to print out the rigid parts. Each rigid part is connected to the next part by autogenous joints without the need for reassembly. This simplifies the fabrication of rigid structural microrobots while improving structural integrity [103].

By observing and analyzing the movement of polypods in nature, researchers found that it is also applicable to the structural design of microrobots. Gu *et al.* achieved metachronal waves in a dynamic magnetic field by specifically preparing the foot of a polypod magnetic microrobot to match the programmed magnetization pattern. This multifooted structure not only achieves efficient motion in fluid environments and on solid surfaces, but also exhibits strong loading and transportation capabilities [104]. In addition, Sun *et al.* further analyzed the motion and control of a magnetic microrobot with a multipedal structure and developed an echinoderm-like multipedal magnetic microrobot. Specific magnetic feet were prepared by an improved method of localization of magnetic powder on the foot. Under the control of the applied magnetic field, the individual control of different rows of feet is realized by using the unevenness of the force of the permanent magnets in the magnetic field, so that its maneuverability and flexibility are further improved [105].

In summary, after continuous research, various structures of magnetic microrobots have been designed to solve or improve the relevant challenges faced. Future magnetic

microrobot structures should also be designed with practical problems in mind to meet operational requirements and enhance operational capabilities.

4 Manufacturing technology of magnetically driven swimming microrobots

As mentioned above, both material and structural differences in magnetically driven microrobots can have an impact on their operation and performance. Micro and nano fabrication technology, the basis of research on magnetic microrobots, also has a significant impact on their operational capabilities. Learning and understanding micro and nano fabrication technology is an important part of magnetic microrobotics research, and to some extent helps to enhance its application potential. The size of magnetically driven microrobots encompasses the span from nanometers to millimeters, and some of them are still complex structures that require sophisticated micromachining techniques to prepare. Thanks to the rapid development of microelectromechanical systems (MEMS) technology, micromachining technology has made great progress in the fields of microfluidics, optical MEMS, RFMEMS, BioMEMS, and its use in nanoMEMS for nanoelectromechanical systems [106]. The main concepts and principles of micromachining are microlithography, ion implantation, thin films, etching, bonding, and polishing. The combination of technologies extends several microfabrication manufacturing techniques that are currently in common use, such as GLAD), DLW, TAED, BTS, photolithography, and self-rolling. In the following subsections, a detailed description of how each method works and its advantages and disadvantages in conjunction with research examples are provided.

4.1 GLAD

Physical vapor deposition (PVD) is the process of transforming a material from a condensed phase to a gas phase and then depositing it onto the surface of a substrate to form a thin film condensed phase. GLAD, as an extension of PVD, employs simultaneous substrate and incidence vapor deposition. It is more suitable for preparing structures with curvature and irregularity by changing the relative positions and angles of the substrates [107,108]. In general, the preparation of magnetic microrobots by GLAD fabrication technology can be generally divided into the following steps. Deposition at an inclined angle of incidence, deposition growth, generation of columnar structures, and columnar structure growth in the direction of incidence (Figure 8a). And, depending on the combination of growth shapes, various shape structures can be generated [51]. Thus, helical magnetic microrobots are usually fabricated by rotating the substrate at a constant speed after growing the initial columnar layer [45,109,110]. Based on this approach, Park *et al.* used silicon nanobeads as a seed layer, and obliquely injecting the deposited material while rotating the substrate, successfully prepared the helical microstructures [48]. Similarly, by tuning the position and rotation speed of the substrate, Wu *et al.* prepared microhelical structures with a specific number of turns [33]. Unlike the random distribution of seed layers on the wafer substrate, Venkataramanababu *et al.* used photolithography prior to depositing the seed layers, forming a patterned wafer for customizing the helical structure of magnetic microrobots [111]. Given the stability of FePt and its availability as a deposited material, the researchers used the GLAD method to prepare the helical structure of the $FePtL1_0$ material (Figure 8b) [112,113]. The micro and nano structures prepared by GLAD technology can be functionalized and coated. Wu *et al.* added a perfluorinated coating to the helical structure prepared by the GLAD technique to reduce adhesion on the surrounding biopolymeric network (Figure 8c). Combining the preparation of micro-sized robots with functionalized processing further increases their operational capabilities [33].

Compared with the embedded distribution of magnetic materials in the microrobot body, the composite body and surface coating prepared using GLAD technology have more stable properties such as corrosion resistance and high-temperature resistance. In addition, the ability of GLAD coatings to be implemented on the surface of many types of materials makes it possible for a single microrobot to have multiple functionalized coatings, which in turn have greater applicability. But again, this method has its own nonnegligible drawbacks, such as the line-of-sight transfer of coating, the need for expensive and highly complex peripherals and control systems, and other typical problems. Taken together, for the preparation of microhelical structures, the GLAD technique is still the better solution in order to ensure process and product accuracy.

4.2 DLW

DLW, also known as multiphoton lithography on polymer templates, eliminates the mask plate and utilizes two-photon absorption to induce changes in the solubility of the resist and developer as compared to normal lithography techniques [114,115]. After determining the characteristic structure

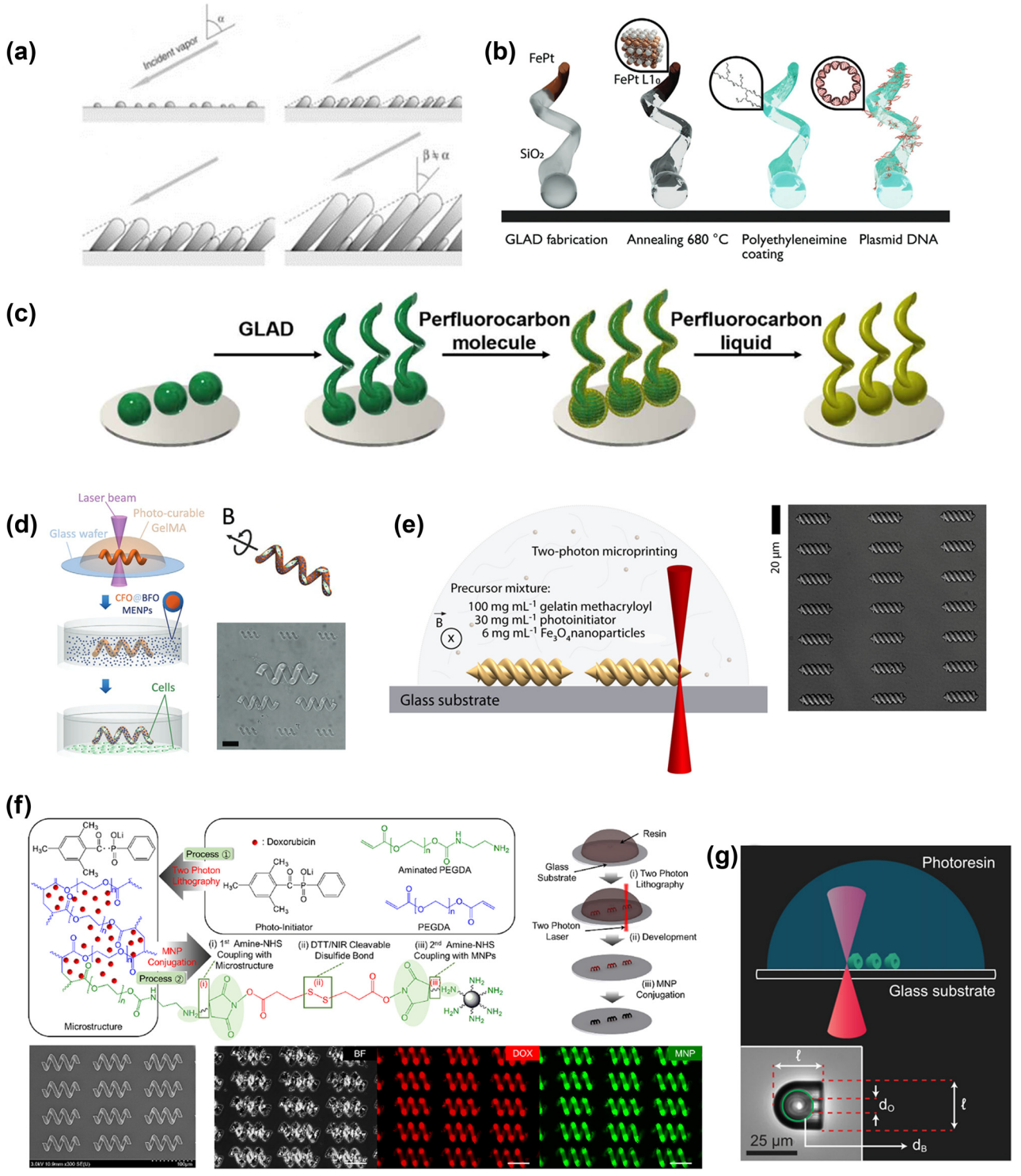

Figure 8: Advanced manufacturing methods commonly used for magnetically driven swimming microrobots. (a) Manufacturing steps of PVD-based GLAD technology. Reproduced from Ref. [51] with permission from Handbook of Deposition Technologies for Films and Coatings. (b) Preparation of $L1_0$ phase magnetic microrobots by deposition of FePt as raw material. Reproduced from Ref. [113] with permission from Adv. Mater. (c) Schematic diagram of microhelical structure preparation using GLAD technology. Reproduced from Ref. [33] with permission from Sci. Adv. (d) Process characterization of magnetic microrobots using TPP technology, and SEM images of microrobots. Reproduced from Ref. [51] with permission from Adv. Funct. Mater. (e) Remodeling of superparamagnetic iron-oxide-based substrates using TPP process, and SEM images of microrobots. Reproduced from Ref. [63] with permission from Acs Nano. (f) The microstructure of encapsulated DOX was prepared by TPL process. Reproduced from Ref. [70] with permission from Acs Appl. Mater. Interfaces. (g) 3D printing of microrobots on slides using TPL technology. Reproduced from Ref. [11] with permission from Proc. Natl Acad. Sci. USA.

for curing, the structure curing is accomplished by irradiating the corresponding photoresist with a light of a definite wavelength, and the commonly used materials are acrylates and photosensitive resins. Wang *et al.* have used the IPL-780 photoresist to prepare micro helical structures by DLW technique. By PVD and surface chemical treatment, they prepared magnetic microrobots with different hydrophobicity [52]. Dong *et al.* used DLW and water dispersion techniques to prepare biodegradable micro helical structures [51]. After further coating the surface with magnetoelectric microparticles, they can be driven by an external magnetic field (Figure 8d). Based on the excellent maneuverability of the helical magnetic microrobots, in order to enhance the surface area of the micro helical structure, the transport capacity is enhanced [35]. Ceylan *et al.* used a two-photon polymerization (TPP) process to prepare the double helix structure (Figure 8e). The configuration of magnetic iron oxide was optimized to improve the volume-to-area ratio [63]. Lee *et al.* used the TPL process to prepare microstructures encapsulated with Doxorubicin Hydrochloride (DOX) drugs. Coupling the aminated MNPs to the disulfide bond makes it biocompatible (Figure 8f) [70]. Aghakhani *et al.* used TPL technology to 3D print microrobotic mechanisms on glass sheets (Figure 8g). Acoustically driven magnetic field-controlled steering, effectively enhances the application [11]. In addition, Li *et al.* designed a new large space burr structure. Using the TPP technique, porous micro-spinel structures were prepared and sputter deposited magnetic materials, which effectively increased the cell transport efficiency [116]. Kim *et al.* based on DLW technique prepared axonal and dendritic microgroove structures. On the basis of having a very high resolution, it can be used as a neuronal cell manipulation tool for cellular transport and neural repair [117].

In the preparation of magnetic microrobots, the DLW technique allows for rapid prototyping of devices with fine feature structures and eliminates the need for complex optical systems. However, a very obvious disadvantage of the DLW technology is that there are fewer biocompatible photosensitive materials that do not meet the requirements for *in vivo* operation of magnetically driven microrobots. After the discovery of compliant light curing materials in the future, DLW technology will be an excellent solution for the preparation of magnetic microrobots.

4.3 BTS

Nature is the great creator, and various organisms have complete structures and rich functions. After the discovery of compliant light curing materials in the future, DLW technology will be an excellent solution for the preparation of magnetic microrobots. This bionic fabrication technology allows magnetic microrobots to be used in biomedical research in a well compatible manner. Wang *et al.*, based on spiral microalgae, used BTS technology to prepare a degradable and highly mobile magnetic microrobot (Figure 9a). The Pd@Au microparticles were electrolytically plated into the Spirulina (Sp.) cell framework and Fe_3O_4 particles were deposited, maintaining structural integrity and response of magnetic field drive [118]. Under specific stimulation, it achieves cargo release and accelerated degradation, enhancing *in vivo* operations. Through an impregnation process, Fe_3O_4 particles are combined with Sp. cells to produce oxygen by photosynthesis under specific stimulation. Relieves hypoxia in tumor cells, enhances the effect of chemotherapy, and aids in the treatment of tumor disease [87]. In addition to allowing photosynthesis to produce oxygen, fluorescent Sp. cells can also be used for tracking *in vivo* movements (Figure 9b) [88]. In addition, sperm cells have an excellent propulsive capacity to release drugs by degradation and are also often used as biological templates [81,119]. Magdanz *et al.* embedded metallic particles in sperm structures for *in vivo* cargo transport by magnetic field actuation and US localization [82].

Due to the simple availability of structural materials, and the high performance of magnetic microrobot design, BTS technology is widely used for the preparation of magnetic microrobots. Then, its disadvantages are obvious. The strength of the biological structure decreases after treatment, and uncontrolled aggregation of decomposition products may occur after *in vivo* manipulation. If more research could be done to ensure the safety of biomaterials for *in vivo* manipulation, the preparation of magnetic microrobots using BTS technology would be the lowest cost micromachining fabrication strategy.

4.4 TAED

TAED is an effective method for preparing magnetic microrobots by electrochemical deposition on prefabricated templates [120]. Due to the low cost, speed, and ease of operation of this deposition technique, it is considered a suitable method for mass production of microstructures. With the help of carefully designed templates, various microstructures have been deposited, including spirals, tubes, rods, *etc*. [121–123].

Anodic aluminum oxide (AAO) is often used as a TAED material for the preparation of nanowire structures.

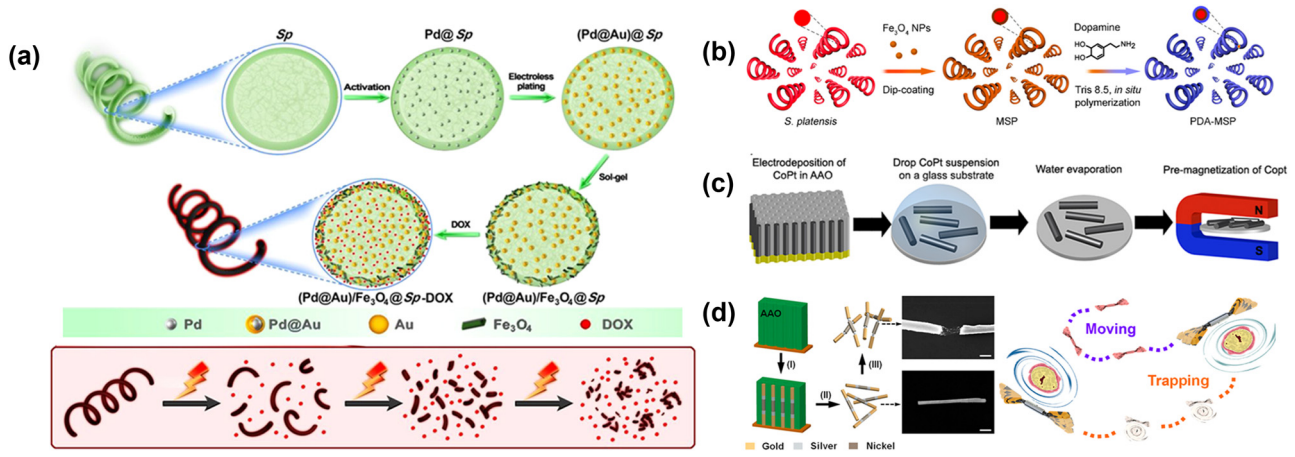

Figure 9: Advanced manufacturing technologies commonly used for magnetically driven swimming microrobots. (a) Schematic diagram of a biohybrid microrobot using BTS technology. Reproduced from Ref. [118] with permission from ACS Appl. Mater. Interfaces. (b) Biohybrid magnetic microrobot using BTS technology to synthesize Fe_3O_4 and Sp. cells separately. Reproduced from Ref. [88] with permission from ACS Nano. (c) Nanowires based on TAED technology, using CoPt-coated demolding and premagnetization process. Reproduced from Ref. [126] with permission from ACS Appl. Mater. Interfaces. (d) Preparation of flexible oscillating magnetic microrobots using TAED technology. Reproduced from Ref. [127] with permission from ACS Nano.

Generally, both sides of the AAO are metallized as working electrodes and then subjected to redox. After deposition of nanowires, the AAO stencil was dissolved. Parameters such as the length of nanostructures prepared by TAED technique are determined based on the electrochemical deposition time. In addition, the prepared nanostructures need to be further magnetized for magnetic drive control [124,125]. However, once the applied magnetic source is removed, the remanent magnetism of the iron and ferromagnetic nanowires comes together on its own. This can be a serious challenge for biomedical applications as it can lead to blood vessel blockage. To solve this issue, Jang *et al.* devised a three stage template preparation method in which the driving magnets are separated by spacer copper and then electrochemically deposited [126]. Based on this approach, Luo *et al.* designed a FeGa@P(VDF-TrFE) biphasic tubular microstructure. The structure is controlled by a magnetic field drive for flexible maneuvering and cargo transportation [3]. In addition, the researchers, based on the AAO stencil demolding and pre-magnetization process, introduced a semi-hard magnetic material (CoPt) to wrap the nanowires (Figure 9c). The prepared magnetic microrobots can tumble, travel, and roll on different rotational frequencies of the rotating magnetic field [126]. Using hinges to connect several template flexibles can increase the degree of freedom of magnetic microrobot motion, thus providing excellent flexibility and better *in vivo* transport (Figure 9d) [127]. Similarly, a multi-segment magnetic microrobot composed of Ni–Ag–Au–Ag–Ni can obtain a velocity of 59.6 $\mu m \cdot s^{-1}$ under an oscillating magnetic field [128]. Although magnetic self-assembly and GLAD techniques are able to fabricate microhelical structures, the number of structural turns is limited. In contrast, with the TAED technique, it is possible to construct long complex 3D structures to provide the corresponding templates [129,130]. Based on this approach, Li *et al.* used the designed polycarbonate membrane as a template and dissolved it with dichloromethane to prepare helical microstructures. Then, sputtered gold modifies its surface layer to generate a negative charge, which adheres the platelet membrane-derived vesicles together and increases their compatibility [130].

Magnetic microrobots with various characteristic structures can be obtained easily and quickly using the TAED technique. However, there is an obvious drawback, that is, it is extremely difficult to design templates for complex structures. The current TAED technology mostly prepares some simple structures, which have to be studied in depth to be widely used in the preparation of magnetic microrobots.

4.5 Other manufacturing technologies

Photolithography is the technique of transferring a pattern on a mask plate to a substrate with the help of a photoresist under the irradiation of light. Moreover, a magnetically driven microrobot, or a mold of a feature structure, can be prepared by a layer-by-layer lithography method. Based on this layer-by-layer lithography approach, Wang *et al.* prepared a bilayer magnetically driven L-shaped microrobot with a nonchiral design using SU-8 photoresist, chitosan,

and Fe_3O_4 [131]. Huang *et al.* developed a lithography method for fabricating helical structures, and the prepared helical magnetic navigation microrobots achieved effective locomotion capabilities in environments with different viscosities [132]. Tan and Cappelleri prepared deformable magnetic hydrogel microrobots using photolithography and TPP techniques with SU-8 as the photoresist and binder and hydrogel and Fe_3O_4 as the body materials, which enhanced. Enhanced its swimming performance and adaptive motion [133]. Photolithography has mature technology products. It is capable of preparing magnetic microrobots at a lower cost and with greater applicability. However, due to its principle of operation, it is possible to damage the mask and photopolymer layer due to the close contact between the mask and the substrate, or to degrade the resolution of the graphic due to the diffraction effect of light.

Self-rolling technology uses different materials deposited on a substrate to self-roll into microstructures by utilizing thermal stress and surface tension in localized areas of the thin layer. Zhang *et al.* prepared Cr/Ni/Au thin films by electron beam evaporation and patterned them by selective etching to self-roll into ABF under localized force control [61]. Zong *et al.* used processed poly(dimethylsiloxane) (PDMS) as a thinness layer to transform multipatterned elastic films into multimodal 3D structures *via* a self-rolling technique [102]. And the self-rolling under different forces was realized, and the multipatterned thin layers were transformed into different microstructures. Self-rolling technology is uniquely suited for transforming thin layers into 3D structures, and is able to impart 3D structural functionality to materials that are biased towards two dimensions. However, due to the limitation of the technical principle, the self-rolling thin layer generally requires other prior steps for processing, which increases the manufacturing steps. In addition, three-dimensional structures made by self-rolling have limited strength, which may lead to structural failure in harsh operating environments.

5 Drive control method for magnetically driven swimming microrobots

Efficient actuation and precise control of magnetically driven microrobots are the focus of research and a critical step towards practical applications. In order to have a more detailed understanding of the current commonly used driving methods and control strategies, as well as the latest research progress, it will be presented in two parts: the driving method and the control strategy.

5.1 Driver methods

Magnetically actuated microrobots are subjected to force F or moment T in a magnetic field, combined with a structural design that results in motion manipulation. The magnetic force and magnetic torque can be obtained from Eqs. (1) and (2). There are two main types of magnetic field sources that have been studied as magnetic drives: The permanent magnets and Maxwell coils for generating gradient fields, and the Helmholtz coils for generating uniform magnetic fields, respectively. Permanent magnets have the advantage of high magnetic field strength and flexible operating range. However, it is commonly used for gradient pulling of magnetic microrobots due to its nonlinear magnetic field strength variation, which leads to poor control accuracy. By receiving a modulation signal from the signal generator, the Maxwell coil is able to effectively control the operating range of the magnetic field gradient. Further, the magnetic field can also be programmed according to the signal generator for versatile manipulation of the magnetic microrobot. Due to its design principle of hollow type, the magnetic field generated by the energized coil is limited, which in turn leads to a small working space. Similar to the way a Maxwell coil operates, a Helmholtz coil receives a signal and produces a uniformly strong field. By adjusting the waveform and frequency of the signal, the angle and period of change of the uniform magnetic field can be changed, thus precisely controlling the motion of the magnetic microrobot. Likewise, it has the typical disadvantages of low magnetic field strength and limited operating space for hollow-core electromagnets.

$$F = V(M\nabla)B, \tag{1}$$

$$T = VM \times B, \tag{2}$$

where B is the flux density, and M and V are the magnetic moment and volume of the magnetic material, respectively.

According to the characteristics of the magnetic field of the field source, the motion of the magnetically driven microrobot can be categorized into gradient pulling by magnetic force and helical propulsion by magnetic torque. Integral rolling is subjected to magnetic torque rotation and other forces, as well as traveling wave and super traveling wave propulsive motions with a mixture of structural and applied forces. Yousefi *et al.* developed a magnetic microrobot control system using four rotating permanent magnets and a pair of Helmholtz coils. The magnetic microrobot is directionally controlled by the torque provided by the Helmholtz coil and is dragged in motion by a rotating magnet that generates a gradient field [134]. Moreover, independent control of two identical magnetic microrobots is

realized based on the tiny size of the microrobots and the relative positional relationship between the individuals. Zhang *et al.* developed a magnetron system with a huge 700 mm × 500 mm × 500 mm workspace using permanent magnets in conjunction with a motor [101]. In the operating space, a permanent magnet generates a gradient field acting on the magnetically guided wire, causing it to drag in a controlled bend. Subjected to the rotating magnetic field of the Helmholtz coil, the helical structure is subjected to a magnetic torque and rotates around its axis, thus converting reciprocating motion into translational motion and realizing helical propulsion. Gong *et al.* prepared spiral magnetic microrobots that can be used to remove Pb(II) from water using a magnetic mixture of modified Spirulina, Fe_3O_4, and MnO_2. Under the driving manipulation of a three-dimensional Helmholtz coil, it shuttles through the wastewater in the form of helical propulsion to achieve a high adsorption capacity of 245.1 $mg \cdot g^{-1}$ [135]. Lee *et al.* developed a helical structured magnetic needle microrobot (MR) by PVD coating nickel (Ni) and titanium dioxide (TiO_2) layers on the helical structure [136]. Driven by an external rotating magnetic field of 20 mT, the MR can reach a helical propulsion speed of 714 μm s^{-1}. Moreover, MR is able to attach to the target microtissue (mT) to achieve continuous drug delivery at the targeted site. A microrobot coated with a magnetic layer on its surface will rotate when subjected to a rotating magnetic field, at which point it will be coupled into a rolling attitude on the surface when in contact with the environmental surface. Schwarz *et al.* designed a magnetic microrobot for transporting fertilized egg spirals (spirals). Under the action of an external rotating magnetic field, the spiral magnetic microrobot moves accordingly along the spatial axis. By further programming the magnetic field, they achieved a "waddling" motion behavior (Figure 10a) [137]. Inspired by leukocytes, Alapan *et al.* prepared micro-rollers for transporting goods in blood vessels with magnetic response. The magnetic micro-roller follows an external rotating magnetic field, and the presence of boundary hydrodynamic forces causes uneven forces on the micro-roller, which converts the rotational motion into rolling along the surface [46]. Lu *et al.* used a tapered multi foot soft foot prepared from a mixture of magnetic particles and PDMS to achieve traveling wave motion through the specific force and transmission of different rows of micropods to the field of a permanent magnet. In addition, this multilimbed microrobot is able to load >100 times its own weight while moving due to its good support and deformation ability. It also has excellent obstacle avoidance capability and is suitable for harsh operating environments [138]. Liao *et al.* developed a magnetic microrobot consisting of multiple rigid sections connected together. Under the external oscillating magnetic field, the vibration of the head is transmitted to the tail through the U-shaped structure of the connecting part, thus realizing traveling wave motion [103]. These motion methods bridge the gap between magnetic fields and the functional design of magnetic microrobots, allowing for more systematic and integrated design and control of magnetic microrobots.

5.2 Control methods

In order to achieve precise and stable motion and localization of magnetic microrobots under the action of magnetic field, it is necessary to adapt and optimize the control strategy in addition to the structural support. These control strategies can include different algorithms, models, and controllers, such as PID control algorithms, optimal bidirectional RRT* models, and SMC controllers. The design of the control strategy is critical because it will directly affect the performance and application range of the microrobot. For example, in the field of biomedicine, it is possible to bring microrobots into the human body for targeted operations only if precise control of them is achieved. Therefore, the design of the control strategy needs to consider factors such as stability, accuracy and real time to meet the requirements of the application scenarios.

Xu *et al.* designed a needle microrobot assembled by magnetic particles with a multimodal motion pattern. The designed motion control strategy realizes the switching of three types of motions: axial motion, lateral motion, and rolling motion. And, after experimental verification of each type of motion, the magnetic particle-assembled microrobot showed better ability to overcome obstacles [37]. Lu *et al.* have designed a robust control system based on the sliding mode control with extended state observer. The block diagram of the control system and the experimental platform are shown in Figure 10b. The path tracking controller is designed to integrate external disturbances into total disturbances for compensation and elimination [139]. Wang *et al.* designed a control system using a handle for remote control. The motion of the magnetic miniature robot is observed by the human eye and the handle sends signals to the external magnetic field for precise manipulation (Figure 10c) [34]. Fan *et al.* proposed a scale-reconfigurable miniature ferromagnetic fluid microrobots (SMFRs) that can reconfigure their morphology in response to external magnetic field stimuli. Based on the design of a multiscale microrobot drive system (M^3RA), a series of control strategies to reconfigure the scale and shape of SMFRs are proposed to realize motion control across scales [140]. Xu *et al.* proposed a control strategy based on a generalized learning system (BLS), which was combined with Lyapunov's theory to

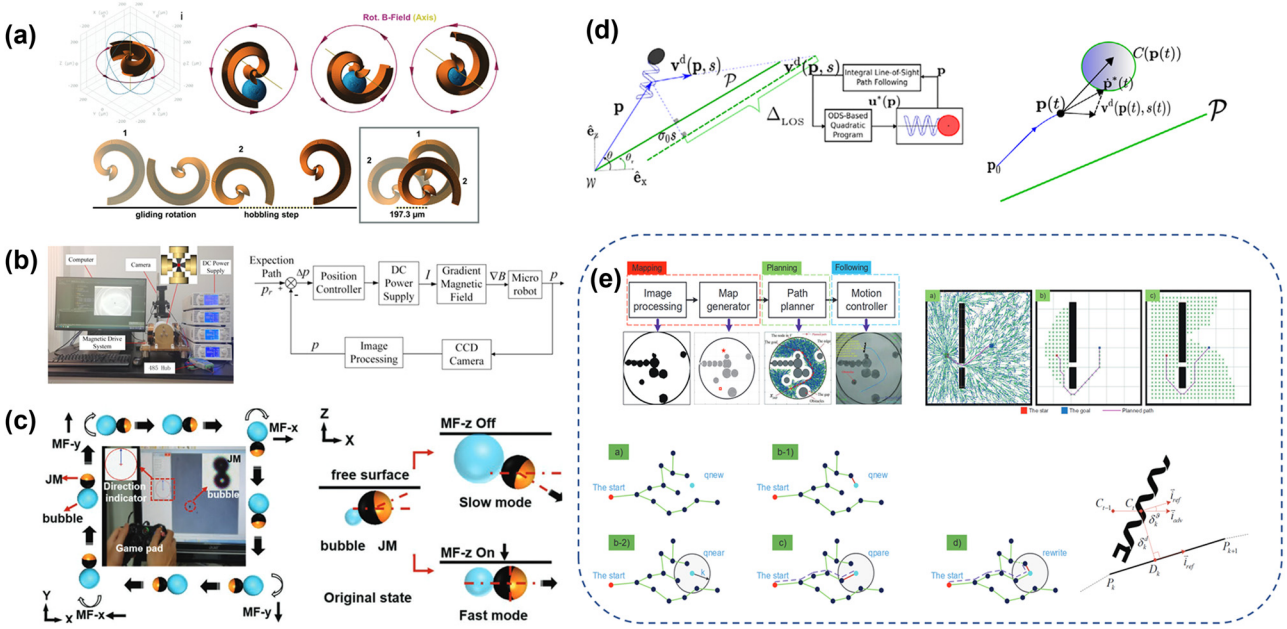

Figure 10: Design of control strategy for magnetically driven swimming microrobots. (a) Schematic diagram of worm helical microrobot motion control principle. Reproduced from Ref. [137] with permission from Advanced Science. (b) Rotating magnetic field drive control, experimental platform with visual feedback, and block diagram of control system. Reproduced from Ref. [139] with permission from Cyborg and Bionic Systems. (c) Remote speed regulation and steering motion of spherical microrobots guided by magnetic field. This figure is reproduced from Ref. [34] with a permission from Small. (d) Block diagram of the line-of-sight reference vector field and ODS-based control scheme, and geometric interpretation of the optimal decision strategy. Reproduced from Ref. [57] with permission from Automatica. (e) Helical microrobot automated manipulation system solution, mapping, planning, and following. Reproduced from Ref. [142] with permission from Micromachines.

obtain constraints on the parameters of a magnetically driven microrobot controller. It is verified by MATLAB simulation and examples with strong generalization and error convergence [141]. This method has simplified the tuning of parameters to the controller while improving the motion accuracy and control performance of the magnetic microrobot. Mohammadi and Spong *et al.* minimizes the discrepancy between the microrobot's velocity and a reference vector field based on the integral line-of-sight (ILOS) according to an optimal decision strategy (ODS), while respecting magnetic saturation constraints and ensuring absolute continuity of the control inputs. Mohammadi and Spong designed a control strategy for a magnetic microrobot based on an ODS by minimizing the difference between the velocity of the microrobot and a reference vector field based on the overall ILOS. During the design process, the magnetic saturation constraints are respected and absolute continuity of the control inputs is ensured to converge to a straight line. The spiral magnetic microrobot linear path tracking problem is solved with better stability (Figure 10d) [57]. Liu *et al.* studied the control of magnetic microrobots in static environments and designed an automatic control system. The system mainly consists of mapper, path planner, and motion controller. The position of magnetic miniature robots and obstacles in free space are marked and the optimal solution is obtained by global path planning algorithm. Then, the motion controller guides magnetic microrobots along the planned path through closed-loop control algorithms (Figure 10e) [142]. Xu *et al.* developed a strategy for manipulating helical magnetic microrobots on low Reynolds liquid surfaces. The control strategy enables the magnetic microrobot to move along a desired path while its body also conforms to a set attitude. And, in order to reduce the external interference, the authors trained a radial basis function network using the reverse propagation algorithm in order to establish the angle compensation model in the global coordinate system [143]. This model can be used to accurately adjust the microrobot's attitude by processing the data collected by the camera, which in turn improves the accuracy and stability of the robot's motion. Liu *et al.* used a BLS neural network to model the input–output relationship between the direction of the magnetic field and the direction of motion of a helical magnetic microrobot, and obtained a motion model of a helical magnetic microrobot. The experimental results show that the average absolute error between the model data and the actual motion is about 3% of the length of the body, and the error is less than 0.5 mm [144]. In addition, Lu *et al.* designed a robust magnetic microrobot control strategy using an extended state observer to estimate the error, and sliding mode control and visual feedback as a controller to compensate the error [139]. Liu *et al.* extended

magnetically driven microrobots to 3D based on path planning and tracking in 2D space. And using neural networks, the compensation angle between the direction of motion and the direction of the magnetic field when the micro-robot is disturbed in 3D space is identified and refined, and the transplantation and updating of the swimming model is realized [145].

A single magnetically driven microrobot, while powerful, is less efficient in its operations. Clustered microrobots have been proposed to solve this problem; however, independent control of multiple microrobots is a great challenge due to the coupling of signals and motion. Cluster control strategies are essential to realize the value of clustered microrobots. Xu *et al.* proposed a strategy for fully decoupled independent control of magnetically driven microrobots by analyzing the relationship between magnetization direction and phase. By analyzing the velocity response curve of the microrobot, the optimal direction of the oscillating magnetic field can be calculated to guide the microbot swarm to generate the desired velocity vector. It was experimentally verified that the control of up to four microbots was successfully realized in terms of independent position control. In addition, the control of up to three microrobots has also been successfully realized in terms of independent path tracking control [146]. The results show that this control strategy has high accuracy and stability and can be applied to a small number of magnetic microbot populations. Yu *et al.* developed a fuzzy control strategy for modulating the pattern deformation, orientation, and position change of elliptical paramagnetic nanoparticle swarms (EPNS). By adjusting the input signal, the morphology of EPNS can be changed [32]. Yang *et al.* proposed a framework for solving environmentally adaptive micro-machine swarm navigation control strategies. A swarm of microbots with different levels of autonomy is used as a unit to design the corresponding system components, and deep learning is utilized to explore the optimal distribution method [147].

6 Application of magnetically driven swimming microrobots

6.1 Targeted drug delivery

Although the development of traditional oral or injectable drug therapy has been widely used in clinical medicine [148], both of these methods are passive methods of *in vivo* drug delivery and may lead to overdosing, which can have side effects on the body [136]. In response to these problems, scientists have developed the concept of targeted drug delivery therapy, which delivers drugs to the location of the lesion for treatment. By dramatically reducing the concentration of the drug, potentially harmful side effects have been reduced. Magnetically driven microrobots, as a typical design for targeted drug delivery, have the advantage of remote, precise, and non-invasive operation. Moreover, it is able to recover carrier residues that adversely affect human tissues and organs [3,67,149]. In addition, the field strengths used to drive magnetic microrobots are typically small, and the effects of magnetically driven fields are minimal compared to those caused by other drive methods [3,150]. It provides a powerful tool for realizing novel therapeutic approaches with targeted drugs [75].

Magnetic microrobots for targeted drug delivery should also be able to perform drug loading and release. There are two main approaches to magnetic microrobot drug loading and release. Encapsulation of the drug inside the magnetic microrobot structure by chemical treatment, or adhesion using the physical properties between the drug and the carrier [21].

Ceylan *et al.* developed a magnetic microrobot that rapidly responds to levels of MMP-2 lyase for biodegradation. The hydrogel absorbs water and swells to degrade, releasing the drug embedded in the magnetic microrobot for targeted drug delivery (Figure 11a) [63]. It is also possible to chemically deposit MNPs and anti-cancer drugs (DOX) attached to the surface of a helical magnetic microrobot. The DOX is delivered to the cancer cell area under a rotating magnetic field. For example, Chen *et al.* designed a spherical magnetic microrobot that deposited DOX Orally into the human body and moved to the target location to release the therapeutic drug under the remote manipulation of an external magnetic field [151]. In addition, magnetic microrobots, biomixed by sperm, can carry anticoagulants for movement in the flowing blood and thus for targeted drug delivery (Figure 11b). It is expected to improve the treatment of circulatory diseases such as blood clots [148]. To reduce the *in vivo* residues of magnetic particles, Lee *et al.* designed a magnetic microrobot that can recover MNP. After completion of DOX delivery, DTT was used as a reducing agent, NIR as an external stimulus to achieve rapid separation and recovery of MNP from the target region (Figure 11c) [70]. This research could reduce the risk of *in vivo* operation of magnetic microrobots and expand the application prospects of magnetically driven swimming microrobots.

6.2 Cell manipulation

Magnetically driven swimming microrobots can achieve manipulation of cells without altering their physiological properties. Schmidt's team designed several magnetic

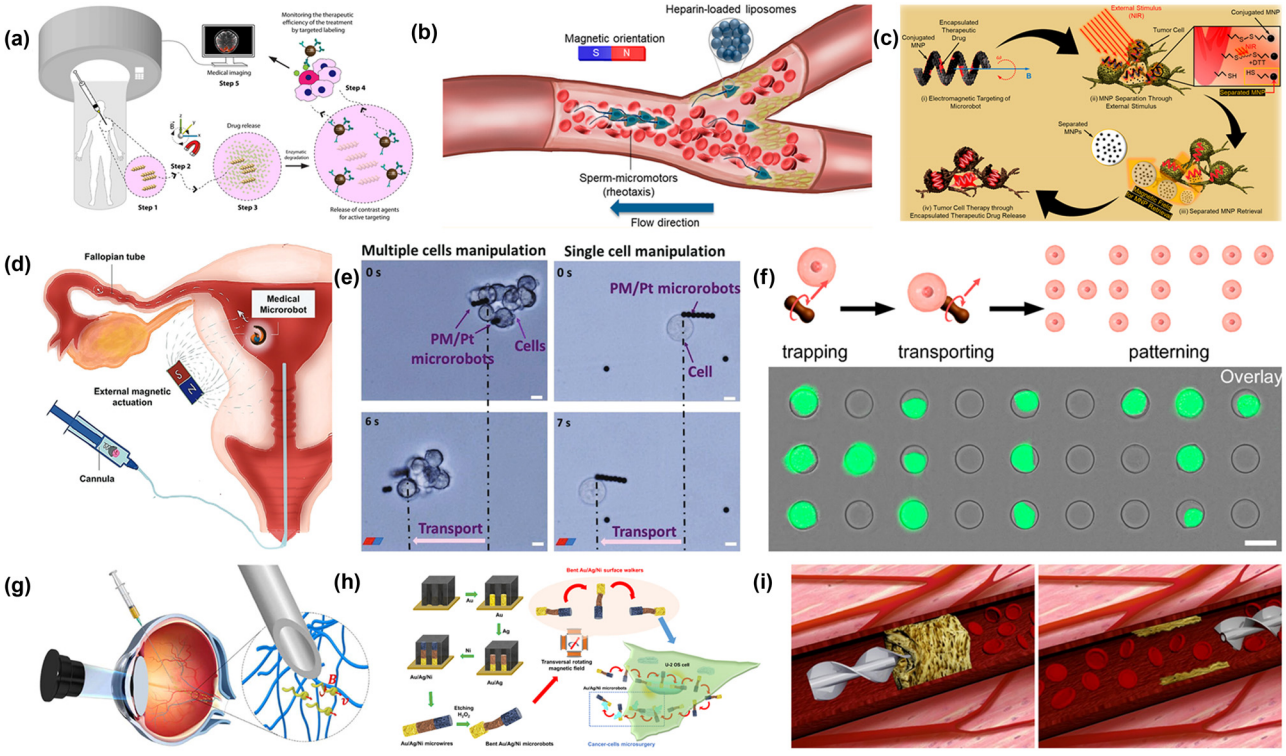

Figure 11: Advanced biotechnology research for targeted drug delivery, minimally invasive surgery, and cell manipulation by magnetically driven roving microrobots. (a) Double helix magnetically driven microrobot for enzymatic biodegradation, concept map for targeted drug delivery applications. Reproduced from Ref. [63] with permission from Acs Nano. (b) Sperm biohybrid microrobots navigate magnetic fields in flowing blood. Reproduced from Ref. [148] with permission from ACS Nano. (c) Magnetically driven microrobot retrieves and clears MNP concept map. Reproduced from Ref. [70] with permission from Acs Appl. Mater. Interfaces. (d) Conceptual diagram of magnetic microrobot-assisted fertilized egg transport. Reproduced from Ref. [137] with permission from Adv. Sci. (e) Bubble driven and magnetic field-controlled navigation for manipulation of single or multiple cells loaded magnetic microrobots. Reproduced from Ref. [152] with permission from Adv. Funct. Mater. (f) External magnetic field drives peanut structured magnetic microrobots that arrange cells in a predetermined pattern. Reproduced from Ref. [153] with permission from ACS Nano. (g) The MagRobots can be injected into the vitreous with the help of magnetic field and optical coherence tomography. Reproduced from Ref. [33] with permission from Sci. Adv. (h) Magnetic microrobotic scalpel penetrates cancer cells, captures a piece of cytoplasm, and leaves the cell while keeping the plasma membrane intact. Reproduced from Ref. [157] with permission from ACS Nano. (i) Schematic diagram of the work of the divisional drill to remove blood clots in a three-dimensional vascular network. Reproduced from Ref. [158] with permission from Nanoscale.

microrobots as aids to assist sperm with motility deficits in the task of fertilization. Magnetic microcarriers with cylindrical cavities enter the manipulation zone *in vivo* and assist sperm movement under the control of an external magnetic field (Figure 11d) [137]. It was shown that based on the chemical reaction that occurs between functional particles on the surface of the organism and the membrane protein moieties of the target cells, it can be used for the capture of breast cancer cells. Based on this theory, Villa *et al.* designed a superparamagnetic PM/Pt microrobot that can bind to amino groups and capture breast cancer cells (Figure 11e) [152]. With the help of the array substrate, the cells were arranged by single cell extraction and delivery using an external magnetic field to propel the peanut structured magnetic microrobot to achieve the predetermined pattern (Figure 11f) [153]. In addition, Kim *et al.* designed a magnetic miniature robot containing nerve cells, with external magnetic fields manipulating the connections of the neural net [117]. Magnetic microrobots made from polylactic acid and functional microclusters improve the efficiency of mesenchymal stem cells (MSCs) delivery in articular cartilage growth. Then, the MSCs will differentiate into new cartilage tissue for therapeutic purposes [154].

6.3 Minimally invasive surgery

The magnetic microrobot is also considered to be a powerful tool for minimally invasive surgery due to its tiny size and excellent maneuverability [155,156]. Fischer's research group designed a helical magnetic microrobot with a smooth surface. The surface is coated with a slippery layer, which minimizes

the adhesion of magnetic microrobots to their surroundings and thus penetrates the cellular biopolymer barrier (Figure 11g) [33]. This microrobot provides a reliable approach to non-invasive ophthalmic treatment. In addition, Vyskočil *et al.* developed an Au/Ag/Ni magnetic microwire with rotational motion under a transverse magnetic field. Concentrated H_2O_2 solution was used to etch part of the Ag segment, giving it the properties of a scalpel. Cleavage, capture, and transport of the cells have been studied [157] (Figure 11h). Magnetic microdrills (tubular Ti/Cr/Fe microdrills with a pointed tip) driven by a magnetic field were able to pass through pig liver tissue cells. Common microdrill robot with tip prepared from biomicrotubules extracted from the edge of the dragon leaf. Magnetically driven microdaggers could penetrate the cell membrane of HeLa cells with a drill like motion, eventually leading to cell death [158]. In addition, due to the good biopermeability of the biological microtubules drilled into the target tissues, joint operation with targeted drug delivery microrobots can be attempted for *in vivo* loading and release of targeted drugs. The millimeter sized magnetic drill can navigate through vascular channels and perforate blood clots in a simulated thrombus model environment, which offers a means of treatment for cardiovascular disease (Figure 11i). These minimally invasive surgery scenarios seem exciting, but it is important to recognize that most of them are *in vitro* simulations of operating environments. To achieve clinical applications and *in vivo* operations, more exploration is needed on the mechanisms, actuation methods, and applications of magnetically driven swimming microrobots in complex biological fluids.

6.4 Other applications

After optimization, magnetically driven swimming microrobots can also be applied to microscopic field sensors, gene delivery, biological biopsies, and cell membrane removal tools for artificial implants. The motion state (speed and oscillation angle) of the magnetically driven swimming microrobot is related to the applied magnetic field, and the properties of the solution (temperature, pH, viscosity, and ionic strength). Thus, magnetically driven swimming microrobot motion state recognition provides a new method for local microenvironment detection in non-homogeneous media [159]. Wang *et al.* developed a helical microrobot mobile viscometer capable of real time monitoring of peripheral viscosity in homogeneous or non-homogeneous media. A summary analysis of the experimental results shows that the contact angle of the helical microrobot in the operating environment varies nonlinearly with the step frequency of the external magnetic field [52]. The microrobot can achieve the detection and evaluation of local performance parameters (viscosity) in complex non-homogeneous media (Figure 12a) [109]. Based on its tiny size and remote precision operation, the magnetically driven swimming microrobot can be used for gene delivery in genetic engineering. Xu *et al.* developed a magnetic microrobot based intracellular delivery nonviral platform for efficient and precise targeted intracellular delivery of high throughput nucleic acids and subcellular in cell culture [160]. Au/Ni silicon oxide microparticles, after being functionalized, are able to penetrate U87 glial cells under the driving control of an external magnetic field and successfully express the carried genes within the cells (Figure 12b). Kadiri *et al.* developed a hard magnet microrobot gene delivery system that balances manufacturing difficulty, biocompatibility, and magnetic particle targeting. The $L1_0$ phase FePt microrobot has excellent magnetic properties for biomedical applications and has experimentally demonstrated targeted cytogenetic transfection of active lung cancer cells (Figure 12c) [113]. This magnetic microrobot mediated transfection allows easy manipulation of multiple cells simultaneously. Moreover, the survival rate of the cells treated by this method is >90% and the gene transfection and expression rate is >80%, which is much higher than the traditional gene manipulation method [161]. Microrobots are important as cell manipulation tools for biosensor and cell engineering analysis. Jin *et al.* developed a magnetic microrobot as a cell engineering manipulation tool that can be manipulated wirelessly to accomplish target tasks. The residual differential stress in the bilayer hinge composed of microrobot silicon oxides acts as a driving force for magnetic layer remote guidance through the narrow catheter and *in vitro* fixed tissue sections (Figure 12d) [162]. Dong *et al.* designed a controllable magnetic microrobot cluster consisting of Fe_3O_4 MNPs. With their remote drive, high cargo capacity and strong local convection, as well as the synergy of chemical and physical processes, the p-Fe_3O_4 magnetic microrobot population could efficiently eliminate biofilms (Figure 12e) [163]. In addition, bacterial biofilm growth on implants such as dental implants can lead to gingivitis, biofilm pathogen infections, implant loss, and expensive care costs. Mayorga *et al.* effectively solved the problem of biofilm erosion contamination on dental implants using photomagnetically active particles as magnetic microrobot [164]. This magnetic microrobot cluster is driven by an external magnetic field and uses $BiVO_4$ as a reactive oxygen generator, and the combined physicochemical action destroys the biofilm colonies (Figure 12f). Sun *et al.* used natural sunflower pollen to design a magnetic sea urchin structured microrobot. The robot is loaded with magnetic droplets that can be used to effectively remove biofilm mixtures attached to biliary endoscopic implants [165]. Driven

by external magnetic fields, the two combine to apply a coercive force that disrupts the tightly adhered biofilm structure on the implant (Figure 12g). The magnetically driven swimming microrobot effectively achieves the disruption of nasty biofilms and ensures the healthy state of artificial implants through efficient cluster operation.

7 Summary, current challenges, and future work

The past decade has seen tremendous advances and breakthroughs in magnetically driven swimming microrobots. These include effective motion design in low Reynolds number environments in the micro-nano domain, novel materials to improve solution feasibility, advanced micro-nano fabrication methods, navigation and tracking control models, and cutting-edge application experiments. Nowadays, these magnetically driven swimming microrobots can perform important tasks in complex biomedical environments. However, there is still a long way to go for practical application in complex biomedical environments, which can be divided into the following areas.

First, most of the materials used for manufacturing magnetic microrobots have certain biological toxicity, and some materials with good biological properties are very expensive. Considering the processing characteristics of the corresponding special materials, all of them greatly limit the development of magnetic microrobots. Second, the current structural design of most magnetic microrobots still needs to satisfy the scallop theory, which leads to simple structure and limited operation capability. Also, from the biological operational point of view, there is a lack of use of "tools," *i.e.*, the ability to collaborate between structures is poor. Third, the micro and nano-fabrication technology for magnetic microrobots still has significant limitations. For instance, microrobots with complex structures can be prepared using GLAD technology, but their operating environments are extremely demanding and the hardware equipment is very expensive. Due to molds, the TAED technique is usually only able to prepare a few simple structures. Lithography related

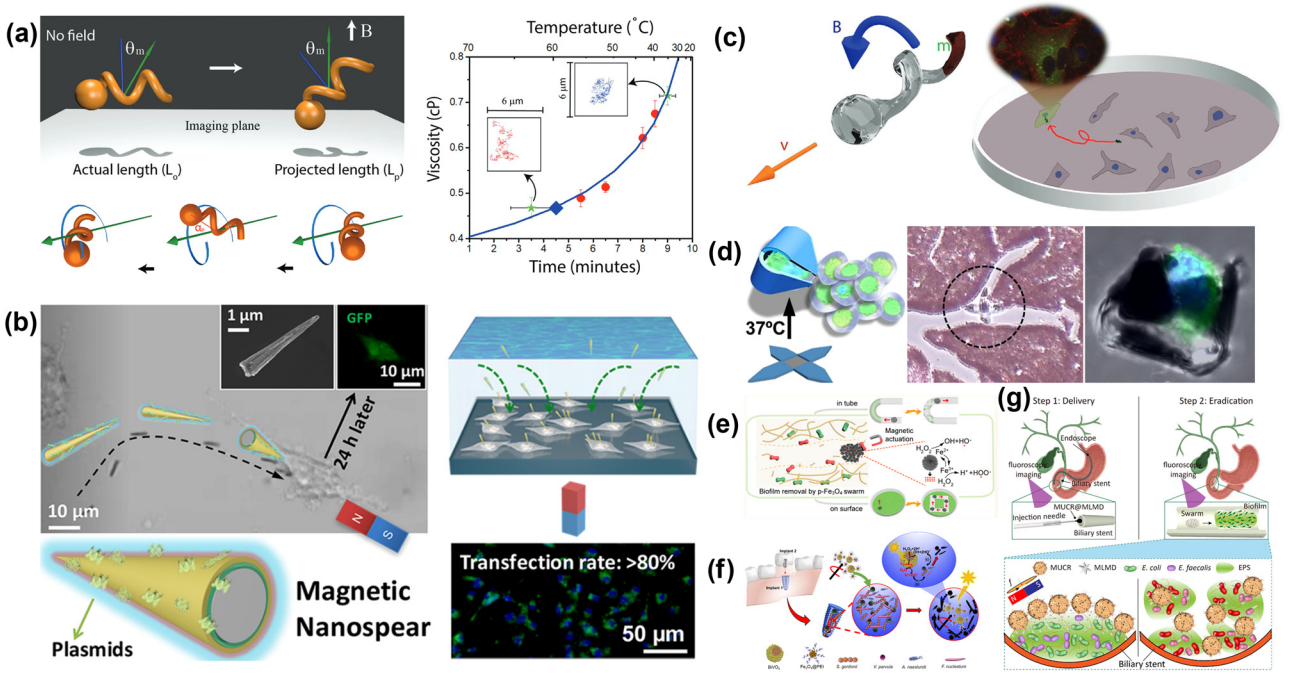

Figure 12: Research on the application of magnetically driven swimming microrobots as sensors, genetic engineering tools, biological biopsies, cell membrane removal, *etc*. (a) Schematic diagram of a microrobot used as a mobile viscometer. Reproduced from Ref. [109] with permission from Adv. Funct. Mater. (b) Schematic diagram of Si/Ni/Au spear structured microrobot operation for targeted intracellular transfection. Reproduced from Ref. [160] with permission from ACS Nano. (c) Schematic diagram of magnetic microrobots for targeted cytogenetic transfection of active lung cancer cells. Reproduced from Ref. [113] with permission from Adv. Mater. (d)Magnetic field navigation and thermally responsive microrobots extract cells from cell clusters for biopsy. Reproduced from Ref. [162] with permission from Nano Lett. (e) Schematic diagram of magnetic microspheres for targeted biofilm decongestion. Reproduced from Ref. [163] with permission from ACS Nano. (f) Schematic diagram of a microrobot cluster for biofilm removal from dental implants. Reproduced from Ref. [164] with permission from ACS Nano. (g) Schematic diagram of microrobot removal of biofilm attached to biliary stent. Reproduced from Ref. [165] with permission from Advanced Materials.

techniques generally require material specificity. All the above problems have affected the development and application of microrobots to some extent. Fourth, the current control strategy for magnetic microrobots is still mainly visual feedback, using camera systems to capture images of microrobot motion, and computer programming to calibrate and identify the images and make feedback corrections according to the planned behavior. Combined with the microrobot application scenarios, the above control methods are too dependent on image acquisition and are not applicable with clinical medical applications. Finally, although current research on magnetic field drive control has yielded tremendous results, it is undeniable that most of the experimental conclusions have been obtained in ideal situations. In the real complex operation environment, there are various disturbances and obstacles. There may be bad situations such as decreased maneuverability of magnetically driven microrobots, difficulty in controlling the direction of motion, or even loss of magnetic microrobot connection.

Accordingly, in order to make magnetic microrobots prosperous and practical applications, it is also necessary to make breakthroughs in these aspects: (i) Continue to develop magnetic microrobot materials with low toxicity, good biocompatibility, and low cost, which meet the prerequisite requirements for clinical applications. (ii) Expanding research on functionalized structural design to increase its functionality and operational capability on the basis of satisfying the basic structural design of magnetic microrobots. For example, using multimodal combinations between structures, the combined magnetic microrobot can be equipped with many different functions, which in turn can enhance the operational capabilities. (iii) Explore new micro and nanofabrication techniques and optimize existing fabrication techniques to increase the feasibility of magnetic microrobot preparation. Or consider using the prepared microrobot as a production tool to go further and prepare more sophisticated and complex structures. (iv) Exploration of clinical devices (*e.g.*, MRI) that can be applied to the magnetic microrobot control system. In addition, as a key step to improve the operational efficiency, it is important to focus on the drive and control strategies of clustered microrobots, and to design precise cluster control or reconfigurable mode switching strategies.

In conclusion, a deep understanding of the mechanism of magnetically driven microrobots and the corresponding influencing factors (*e.g.*, materials, geometry, fabrication technology, and control strategy) is a prerequisite for realistic, functional, and automated magnetic robots. Good biocompatibility, high mobility in the operating space, precision in manipulation, and functional design effectiveness are the ultimate research goals of magnetic microrobots. Standing at the transition stage where magnetic microrobots are taking the lead in moving from the laboratory to clinical applications, we believe that all of this, eventually, will be practically applied.

Acknowledgments: The authors wish to acknowledge the foundations and all co-authors.

Funding information: The authors wish to acknowledge the funding provided by the National Natural Science Foundation of China (Project No. 62273289) and The Youth Innovation Science and Technology Support Program of Shandong Province (Project No.2022KJ274).

Author contributions: All authors have accepted responsibility for the entire content of this manuscript and approved its submission.

Conflict of interest: The authors state no conflict of interest.

Data availability statement: All data generated or analyzed during this study are included in this published article.

References

[1] Kucuk, S. Introductory chapter: medical robots in surgery and rehabilitation. In: *Medical Robotics - New Achievements*, K. Serdar, Abdullah Erdem, C., editors, IntechOpen, Rijeka, 2020, id. Ch. 1.

[2] Li, J., E. S. Barjuei, G. Ciuti, Y. Hao, P. Zhang, A. Menciassi, et al. Magnetically-driven medical robots: An analytical magnetic model for endoscopic capsules design. *Journal of Magnetism and Magnetic Materials*, Vol. 452, 2018, pp. 278–287.

[3] Luo, M., Y. Z. Feng, T. W. Wang, and J. G. Guan. Micro-/nanorobots at work in active drug delivery. *Advanced Functional Materials*, Vol. 28, No. 25, 2018, id. 1706100.

[4] Sitti, M. and D. S. Wiersma. Pros and Cons: Magnetic *versus* Optical Microrobots. *Advanced Materials*, Vol. 32, No. 20, 2020, id. 1906766.

[5] Yamanaka, T. and F. Arai. Self-propelled swimming microrobot using electroosmotic propulsion and biofuel cell. *IEEE Robotics and Automation Letters*, Vol. 3, No. 3, 2018, pp. 1787–1792.

[6] Kim, D. and S. Ahn. Wireless power transfer-based microrobot with magnetic force propulsion considering power transfer efficiency. *Journal of Electromagnetic Engineering and Science*, Vol. 22, No. 4, 2022, pp. 488–495.

[7] Sridhar, V., F. Podjaski, J. Kröger, A. Jiménez-Solano, B.-W. Park, B. V. Lotsch, et al. Carbon nitride-based light-driven microswimmers with intrinsic photocharging ability. *Proceedings of the National Academy of Sciences*, Vol. 117, No. 40, 2020, pp. 24748–24756.

[8] Pourrahimi, A. M., K. Villa, C. L. Manzanares Palenzuela, Y. Ying, Z. Sofer, and M. Pumera. Catalytic and light-driven ZnO/Pt Janus nano/micromotors: Switching of motion mechanism via interface roughness and defect tailoring at the nanoscale. *Advanced Functional Materials*, Vol. 29, No. 22, 2019, id. 1808678.

[9] Ying, Y., A. M. Pourrahimi, C. L. Manzanares-Palenzuela, F. Novotny, Z. Sofer, and M. Pumera. Light-driven ZnO brush-shaped self-propelled micromachines for nitroaromatic explosives decomposition. *Small*, Vol. 16, No. 27, 2020, id. 1902944.

[10] Go, G., V. D. Nguyen, Z. Jin, J.-O. Park, and S. Park. A thermo-electromagnetically actuated microrobot for the targeted transport of therapeutic agents. *International Journal of Control, Automation and Systems*, Vol. 16, No. 3, 2018, pp. 1341–1354.

[11] Aghakhani, A., O. Yasa, P. Wrede, and M. Sitti. Acoustically powered surface-slipping mobile microrobots. *Proceedings of the National Academy of Sciences*, Vol. 117, No. 7, 2020, pp. 3469–3477.

[12] Esteban-Fernández de Ávila, B., P. Angsantikul, D. E. Ramírez-Herrera, F. Soto, H. Teymourian, D. Dehaini, et al. Hybrid biomembrane-functionalized nanorobots for concurrent removal of pathogenic bacteria and toxins. *Science Robotics*, Vol. 3, No. 18, 2018, id. eaat0485.

[13] Ren, L., N. Nama, J. M. McNeill, F. Soto, Z. Yan, W. Liu, et al. 3D steerable, acoustically powered microswimmers for single-particle manipulation. *Science Advances*, Vol. 5, No. 10, 2019, id. eaax3084.

[14] Mirkovic, T., N. S. Zacharia, G. D. Scholes, and G. A. Ozin. Fuel for thought: Chemically powered nanomotors out-swim nature's flagellated bacteria. *ACS Nano*, Vol. 4, No. 4, 2010, pp. 1782–1789.

[15] Sánchez, S., L. Soler, and J. Katuri. Chemically Powered Micro- and Nanomotors. *Angewandte Chemie International Edition*, Vol. 54, No. 5, 2015, pp. 1414–1444.

[16] Kong, L., N. F. Rosli, H. L. Chia, J. Guan, and M. Pumera. Self-propelled autonomous Mg/Pt Janus micromotor interaction with human cells. *Bulletin of the Chemical Society of Japan*, Vol. 92, No. 10, 2019, pp. 1754–1758.

[17] Patiño, T., X. Arqué, R. Mestre, L. Palacios, and S. Sánchez. Fundamental aspects of enzyme-powered micro- and nanoswimmers. *Accounts of Chemical Research*, Vol. 51, No. 11, 2018, pp. 2662–2671.

[18] Alapan, Y., O. Yasa, B. Yigit, I. C. Yasa, P. Erkoc, and M. Sitti. Microrobotics and microorganisms: Biohybrid autonomous cellular robots. *Annual Review of Control, Robotics, and Autonomous Systems*, Vol. 2, No. 1, 2019, pp. 205–230.

[19] Mostaghaci, B., O. Yasa, J. Zhuang, and M. Sitti. Bioadhesive bacterial microswimmers for targeted drug delivery in the urinary and gastrointestinal tracts. *Advanced Science*, Vol. 4, No. 6, 2017, id. 1700058.

[20] Vizsnyiczai, G., G. Frangipane, C. Maggi, F. Saglimbeni, S. Bianchi, and R. Di Leonardo. Light controlled 3D micromotors powered by bacteria. *Nature Communications*, Vol. 8, No. 1, 2017, id. 15974.

[21] Zhou, H., C. C. Mayorga-Martinez, S. Pané, L. Zhang, and M. Pumera. Magnetically driven micro and nanorobots. *Chemical Reviews*, Vol. 121, No. 8, 2021, pp. 4999–5041.

[22] Yang, J., C. Zhang, X. D. Wang, W. X. Wang, N. Xi, and L. Q. Liu. Development of micro- and nanorobotics: A review. *Science China Technological Sciences*, Vol. 62, No. 1, 2019, pp. 1–20.

[23] Purcell, E. M. Life at low Reynolds number. *American Journal of Physics*, Vol. 45, No. 1, 1977, pp. 3–11.

[24] Goodchild, M. F. and D. C. Ford. Analysis of scallop patterns by simulation under controlled conditions. *The Journal of Geology*, Vol. 79, No. 1, 1971, pp. 52–62.

[25] Yang, L., X. X. Chen, L. Wang, Z. J. Hu, C. Xin, M. Hippler, et al. Targeted single-cell therapeutics with magnetic tubular micromotor by one-step exposure of structured femtosecond optical vortices. *Advanced Functional Materials*, Vol. 29, No. 45, 2019, id. 1905745.

[26] Liu, Y., D. Ge, J. Cong, H. G. Piao, X. Huang, Y. Xu, et al. Magnetically powered annelid-worm-like microswimmers. *Small*, Vol. 14, No. 17, 2018, id. e1704546.

[27] Hu, N. R., L. F. Wang, W. H. Zhai, M. M. Sun, H. Xie, Z. G. Wu, et al. Magnetically actuated rolling of star-shaped hydrogel microswimmer. *Macromolecular Chemistry and Physics*, Vol. 219, No. 5, 2018, id. 1700540.

[28] Tang, Y., M. Li, T. Wang, X. Dong, W. Hu, and M. Sitti. Wireless miniature magnetic phase-change soft actuators. *Advanced Materials*, Vol. 34, No. 40, 2022, id. e2204185.

[29] Wang, H., S. Yu, J. Liao, X. Qing, D. Sun, F. Ji, et al. A robot platform for highly efficient pollutant purification. *Frontiers in Bioengineering and Biotechnology*, Vol. 10, 2022, id. 903219.

[30] Zhu, S., Y. Cheng, J. Chen, G. Liu, T. Luo, and R. Yang. Dynamically reversible cooperation and interaction of multiple rotating micromotors. *Lab on a Chip*, Vol. 23, No. 7, 2023, pp. 1905–1917.

[31] Law, J., H. Chen, Y. Wang, J. Yu, and Y. Sun. Gravity-resisting colloidal collectives. *Science Advances*, Vol. 8, No. 46, 2022, id. eade3161.

[32] Yu, J., L. Yang, X. Du, H. Chen, T. Xu, and L. Zhang. Adaptive pattern and motion control of magnetic microrobotic swarms. *IEEE Transactions on Robotics*, Vol. 38, No. 3, 2022, pp. 1552–1570.

[33] Wu, Z., J. Troll, H. H. Jeong, Q. Wei, M. Stang, F. Ziemssen, et al. A swarm of slippery micropropellers penetrates the vitreous body of the eye. *Science Advances*, Vol. 4, No. 11, 2018, id. eaat4388.

[34] Wang, L., L. Chen, X. Zheng, Z. Yu, W. Lv, M. Sheng, et al. Multimodal bubble microrobot near an air–water interface. *Small*, Vol. 18, No. 39, 2022, id. 2203872.

[35] Jeon, S., S. Kim, S. Ha, S. Lee, E. Kim, S. Y. Kim, et al. Magnetically actuated microrobots as a platform for stem cell transplantation. *Science Robotics*, Vol. 4, No. 30, 2019, id. eaav4317.

[36] Coey, J. M. D. Magnetic materials. *Journal of Alloys and Compounds*, Vol. 326, No. 1–2, 2001, pp. 2–6.

[37] Xu, T., Z. Hao, C. Huang, J. Yu, L. Zhang, and X. Wu. Multimodal locomotion control of needle-like microrobots assembled by ferromagnetic nanoparticles. *IEEE/ASME Transactions on Mechatronics*, Vol. 27, No. 6, 2022, pp. 4327–4338.

[38] Zhu, H., Y. He, Y. Wang, Y. Zhao, and C. Jiang. Mechanically-guided 4D printing of magnetoresponsive soft materials across different length scale. *Advanced Intelligent Systems*, Vol. 4, No. 3, 2022, id. 2100137.

[39] Givord D. Introduction to Magnetism and Magnetic Materials. In: Beaurepaire E, Kappler JP, Krill G, Scheurer F, editors. Magnetism and Synchrotron Radiation. Berlin, Heidelberg: Springer Berlin Heidelberg; 2001. p. 3–23.

[40] Yu, J. F., T. T. Xu, Z. Y. Lu, C. I. Vong, and L. Zhang. On-demand disassembly of paramagnetic nanoparticle chains for microrobotic cargo delivery. *IEEE Transactions on Robotics*, Vol. 33, No. 5, 2017, pp. 1213–1225.

[41] Jang, B., E. Gutman, N. Stucki, B. F. Seitz, P. D. Wendel-Garcia, T. Newton, et al. Undulatory locomotion of magnetic multilink nanoswimmers. *Nano Letters*, Vol. 15, No. 7, 2015, pp. 4829–4833.

[42] Li, S., D. Liu, Y. Hu, Z. Su, X. Zhang, R. Guo, et al. Soft magnetic microrobot doped with porous silica for stability-enhanced multimodal locomotion in a nonideal environment. *ACS Applied Materials & Interfaces*, Vol. 14, No. 8, 2022, pp. 10856–10874.

[43] Darmawan, B. A., D. Gong, H. Park, S. Jeong, G. Go, S. Kim, et al. Magnetically controlled reversible shape-morphing microrobots with real-time X-ray imaging for stomach cancer applications. *Journal of Materials Chemistry B*, Vol. 10, No. 23, 2022, pp. 4509–4518.

[44] Gu, H., M. Möckli, C. Ehmke, M. Kim, M. Wieland, S. Moser, et al. Self-folding soft-robotic chains with reconfigurable shapes and functionalities. *Nature Communications*, Vol. 14, No. 1, 2023, id. 1263.

[45] Ye, C., J. Liu, X. Wu, B. Wang, L. Zhang, Y. Zheng, et al. Hydrophobicity influence on swimming performance of magnetically driven miniature helical swimmers. *Micromachines (Basel)*, Vol. 10, No. 3, 2019, id. 175.

[46] Alapan, Y., U. Bozuyuk, P. Erkoc, A. C. Karacakol, and M. Sitti. Multifunctional surface microrollers for targeted cargo delivery in physiological blood flow. *Science Robotics*, Vol. 5, No. 42, 2020, id. eaba5726.

[47] Yasa, O., P. Erkoc, Y. Alapan, and M. Sitti. Microalga-powered microswimmers toward active cargo delivery. *Advanced Materials*, Vol. 30, No. 45, 2018, id. 1804130.

[48] Park, J., C. Jin, S. Lee, J. Y. Kim, and H. Choi. Magnetically actuated degradable microrobots for actively controlled drug release and hyperthermia therapy. *Advanced Healthcare Materials*, Vol. 8, No. 16, 2019, id. e1900213.

[49] Gao, C., Z. Lin, D. Wang, Z. Wu, H. Xie, and Q. He. Red blood cell-mimicking micromotor for active photodynamic cancer therapy. *ACS Applied Materials & Interfaces*, Vol. 11, No. 26, 2019, pp. 23392–23400.

[50] Sun, M., X. Fan, X. Meng, J. Song, W. Chen, L. Sun, et al. Magnetic biohybrid micromotors with high maneuverability for efficient drug loading and targeted drug delivery. *Nanoscale*, Vol. 11, No. 39, 2019, pp. 18382–18392.

[51] Dong, M., X. P. Wang, X. Z. Chen, F. Mushtaq, S. Y. Deng, C. H. Zhu, et al. 3D-printed soft magnetoelectric microswimmers for delivery and differentiation of neuron-like cells. *Advanced Functional Materials*, Vol. 30, No. 17, 2020, id. 1910323.

[52] Wang, X., C. Hu, L. Schurz, C. De Marco, X. Chen, S. Pané, et al. Surface-chemistry-mediated control of individual magnetic helical microswimmers in a swarm. *ACS Nano*, Vol. 12, No. 6, 2018, pp. 6210–6217.

[53] Wang, C., A. Mzyk, R. Schirhagl, S. Misra, and V. K. Venkiteswaran. Biocompatible film-coating of magnetic soft robots for mucoadhesive locomotion. *Advanced Materials Technologies-Us*, Vol. 8, No. 12, 2023, id. 2201813.

[54] Li, M., J. Wu, D. Lin, J. Yang, N. Jiao, Y. Wang, et al. A diatom-based biohybrid microrobot with a high drug-loading capacity and pH-sensitive drug release for target therapy. *Acta Biomaterialia*, Vol. 154, 2022, pp. 443–453.

[55] Ye, M., Y. Zhou, H. Zhao, and X. Wang. Magnetic Microrobots with Folate Targeting for Drug Delivery. *Cyborg and Bionic Systems*, Vol. 4, 2023, id. 0019.

[56] Shen, H., S. Cai, Z. Wang, Z. Ge, and W. Yang. Magnetically driven microrobots: Recent progress and future development. *Materials & Design*, Vol. 227, 2023, id. 111735.

[57] Mohammadi, A. and M. W. Spong. Integral line-of-sight path following control of magnetic helical microswimmers subject to step-out frequencies. *Automatica*, Vol. 128, 2021, id. 109554.

[58] Samsami, K., S. A. Mirbagheri, F. Meshkati, and H. C. Fu. Stability of soft magnetic helical microrobots. *Fluids*, Vol. 5, No. 1, 2020, id. 19.

[59] Li, T., X. Chang, Z. Wu, J. Li, G. Shao, X. Deng, et al. Autonomous collision-free navigation of microvehicles in complex and dynamically changing environments. *ACS Nano*, Vol. 11, No. 9, 2017, pp. 9268–9275.

[60] Xu, T. T., J. F. Yu, C. I. Vong, B. Wang, X. Y. Wu, and L. Zhang. Dynamic morphology and swimming properties of rotating miniature swimmers with soft tails. *IEEE/ASME Transactions on Mechatronics*, Vol. 24, No. 3, 2019, pp. 924–934.

[61] Zhang, L., J. J. Abbott, L. Dong, B. E. Kratochvil, D. Bell, and B. J. Nelson. Artificial bacterial flagella: Fabrication and magnetic control. *Applied Physics Letters*, Vol. 94, 2009, id. 064107.

[62] Xu, H., M. Medina-Sanchez, and O. G. Schmidt. Magnetic micromotors for multiple motile sperm cells capture, transport, and enzymatic release. *Angewandte Chemie-International Edition in English*, Vol. 59, No. 35, 2020, pp. 15029–15037.

[63] Ceylan, H., I. C. Yasa, O. Yasa, A. F. Tabak, J. Giltinan, and M. Sitti. 3D-printed biodegradable microswimmer for theranostic cargo delivery and release. *ACS Nano*, Vol. 13, No. 3, 2019, pp. 3353–3362.

[64] Huang, H. W., T. Y. Huang, M. Charilaou, S. Lyttle, Q. Zhang, S. Pane, et al. Investigation of Magnetotaxis of Reconfigurable Micro-Origami Swimmers with Competitive and Cooperative Anisotropy. *Advanced Functional Materials*, Vol. 28, No. 36, 2018, id. 1802110.

[65] Zheng, Z., H. Wang, S. O. Demir, Q. Huang, T. Fukuda, and M. Sitti. Programmable aniso-electrodeposited modular hydrogel microrobots. *Science Advances*, Vol. 8, No. 50, 2022, id. eade6135.

[66] Sokolich, M., D. Rivas, Y. Yang, M. Duey, and S. Das. ModMag: A modular magnetic micro-robotic manipulation device. *MethodsX*, Vol. 10, 2023, id. 102171.

[67] Iacovacci, V., L. Ricotti, G. Signore, F. Vistoli, E. Sinibaldi, and A. Menciassi. Retrieval of magnetic medical microrobots from the bloodstream. *International Conference on Robotics and Automation*, 2019, pp. 2495–2501.

[68] Kim, D. I., H. Lee, S. H. Kwon, H. Choi, and S. Park. Magnetic nanoparticles retrievable biodegradable hydrogel microrobot. *Sensor Actuator B-Chemistry*, Vol. 289, 2019, pp. 65–77.

[69] Kim, D. I., H. Lee, S. H. Kwon, Y. J. Sung, W. K. Song, and S. Park. Bilayer hydrogel sheet-type intraocular microrobot for drug delivery and magnetic nanoparticles retrieval. *Advanced Healthcare Materials*, Vol. 9, No. 13, 2020, id. e2000118.

[70] Lee, H., D. I. Kim, S. H. Kwon, and S. Park. Magnetically actuated drug delivery helical microrobot with magnetic nanoparticle retrieval ability. *ACS Applied Materials & Interfaces*, Vol. 13, No. 17, 2021, pp. 19633–19647.

[71] Esteban-Fernandez de Avila, B., W. Gao, E. Karshalev, L. Zhang, and J. Wang. Cell-like micromotors. *Accounts of Chemical Research*, Vol. 51, No. 9, 2018, pp. 1901–1910.

[72] Palagi, S. and P. Fischer. Bioinspired microrobots. *Nature Reviews Materials*, Vol. 3, No. 6, 2018, pp. 113–124.

[73] Ricotti, L., B. Trimmer, A. W. Feinberg, R. Raman, K. K. Parker, R. Bashir, et al. Biohybrid actuators for robotics: A review of devices actuated by living cells. *Science Robotics*, Vol. 2, No. 12, 2017.

[74] Sun, L., Y. Yu, Z. Chen, F. Bian, F. Ye, L. Sun, et al. Biohybrid robotics with living cell actuation. *Chemical Society Reviews*, Vol. 49, No. 12, 2020, pp. 4043–4069.

[75] Choi, J., J. Hwang, J. Y. Kim, and H. Choi. Recent progress in magnetically actuated microrobots for targeted delivery of therapeutic agents. *Advanced Healthcare Materials*, Vol. 10, No. 6, 2021, id. e2001596.

[76] Erkoc, P., I. C. Yasa, H. Ceylan, O. Yasa, Y. Alapan, and M. Sitti. Mobile microrobots for active therapeutic delivery. *Advanced Therapeutics-Germany*, Vol. 2, No. 1, 2019, id. 1800064.

[77] Guo, J., J. O. Agola, R. Serda, S. Franco, Q. Lei, L. Wang, et al. Biomimetic rebuilding of multifunctional red blood cells: modular design using functional components. *ACS Nano*, Vol. 14, No. 7, 2020, pp. 7847–7859.

[78] Nguyen, V. D., J. Han, G. Go, J. Zhen, S. Zheng, V. H. Le, et al. Feasibility study of dual-targeting paclitaxel-loaded magnetic liposomes using electromagnetic actuation and macrophages. *Sensors and Actuators B: Chemical*, Vol. 240, 2017, pp. 1226–1236.

[79] Magdanz, V., M. Medina-Sanchez, L. Schwarz, H. Xu, J. Elgeti, and O. G. Schmidt. Spermatozoa as functional components of robotic microswimmers. *Advanced Materials*, Vol. 29, No. 24, 2017, id. 1606301.

[80] Striggow, F., M. Medina-Sanchez, G. K. Auernhammer, V. Magdanz, B. M. Friedrich, and O. G. Schmidt. Sperm-driven micromotors moving in oviduct fluid and viscoelastic media. *Small*, Vol. 16, No. 24, 2020, id. e2000213.

[81] Xu, H., M. Medina-Sanchez, V. Magdanz, L. Schwarz, F. Hebenstreit, and O. G. Schmidt. Sperm-hybrid micromotor for targeted drug delivery. *ACS Nano*, Vol. 12, No. 1, 2018, pp. 327–337.

[82] Magdanz, V., I. S. M. Khalil, J. Simmchen, G. P. Furtado, S. Mohanty, J. Gebauer, et al. IRONSperm: Sperm-templated soft magnetic microrobots. *Science Advances*, Vol. 6, No. 28, 2020, id. eaba5855.

[83] Maric, T., M. Z. M. Nasir, N. F. Rosli, M. Budanovic, R. D. Webster, N. J. Cho, et al. Microrobots derived from variety plant pollen grains for efficient environmental clean up and as an anti-cancer drug carrier. *Advanced Functional Materials*, Vol. 30, No. 19, 2020, id. 2000112.

[84] Prabhakar, A. K., M. G. Potroz, E. L. Tan, H. Jung, J. H. Park, and N. J. Cho. Macromolecular microencapsulation using pine pollen: Loading optimization and controlled release with natural materials. *ACS Applied Materials & Interfaces*, Vol. 10, No. 34, 2018, pp. 28428–28439.

[85] Zhang, Y., L. Zhang, L. Yang, C. I. Vong, K. F. Chan, W. K. K. Wu, et al. Real-time tracking of fluorescent magnetic spore-based microrobots for remote detection of *C. diff* toxins. *Science Advances*, Vol. 5, No. 1, 2019, id. eaau9650.

[86] Liu, L., B. Chen, K. Liu, J. B. Gao, Y. C. Ye, Z. Wang, et al. Wireless manipulation of magnetic/piezoelectric micromotors for precise neural stem-like cell stimulation. *Advanced Functional Materials*, Vol. 30, No. 11, 2020, id. 1910108.

[87] Zhong, D. N., W. L. Li, Y. C. Qi, J. He, and M. Zhou. Photosynthetic biohybrid nanoswimmers system to alleviate tumor hypoxia for FL/PA/MR imaging-guided enhanced radio-photodynamic synergetic therapy. *Advanced Functional Materials*, Vol. 30, No. 17, 2020, id. 1910395.

[88] Xie, L., X. Pang, X. Yan, Q. Dai, H. Lin, J. Ye, et al. Photoacoustic imaging-trackable magnetic microswimmers for pathogenic bacterial infection treatment. *ACS Nano*, Vol. 14, No. 3, 2020, pp. 2880–2893.

[89] Yan, X., Q. Zhou, M. Vincent, Y. Deng, J. Yu, J. Xu, et al. Multifunctional biohybrid magnetite microrobots for imaging-guided therapy. *Science Robotics*, Vol. 2, No. 12, 2017. id. eaaq1155.

[90] Bhalla, S., D. T. Melnekoff, A. Aleman, V. Leshchenko, P. Restrepo, J. Keats, et al. Patient similarity network of newly diagnosed multiple myeloma identifies patient subgroups with distinct genetic features and clinical implications. *Science Advances*, Vol. 7, No. 47, 2021, id. eabg9551.

[91] Folio, D. and A. Ferreira. Modeling and estimation of self-phoretic magnetic Janus microrobot with uncontrollable inputs. *IEEE Transactions on Control Systems Technology*, Vol. 30, No. 6, 2022, pp. 2681–2688.

[92] Campuzano, S., M. Gamella, V. Serafín, M. Pedrero, P. Yáñez-Sedeño, and J. M. Pingarrón. Magnetic Janus particles for static and dynamic (bio)sensing. *Magnetochemistry*, Vol. 5, No. 3, 2019, id. 47.

[93] Feng, Z. Q., K. Yan, J. Li, X. Xu, T. Yuan, T. Wang, et al. Magnetic Janus particles as a multifunctional drug delivery system for paclitaxel in efficient cancer treatment. *Materials Science and Engineering: C. Materials for Biological Applications*, Vol. 104, 2019, id. 110001.

[94] Yuan, K. S., V. de la Asuncion-Nadal, B. Jurado-Sanchez, and A. Escarpa. 2D nanomaterials wrapped Janus micromotors with built-in multiengines for bubble, magnetic, and light driven propulsion. *Chemistry of Materials*, Vol. 32, No. 5, 2020, pp. 1983–1992.

[95] Li, T., A. Zhang, G. Shao, M. Wei, B. Guo, G. Zhang, et al. Janus microdimer surface walkers propelled by oscillating magnetic fields. *Advanced Functional Materials*, Vol. 28, No. 25, 2018, id. 1706066.

[96] Yu, S., T. Li, F. Ji, S. Zhao, K. Liu, Z. Zhang, et al. Trimer-like microrobots with multimodal locomotion and reconfigurable capabilities. *Materials Today Advances*, Vol. 14, 2022, id. 100231.

[97] Jin, D., J. Yu, K. Yuan, and L. Zhang. Mimicking the structure and function of ant bridges in a reconfigurable microswarm for electronic applications. *ACS Nano*, Vol. 13, No. 5, 2019, pp. 5999–6007.

[98] Xu, B. R., B. R. Zhang, L. Wang, G. S. Huang, and Y. F. Mei. Tubular micro/nanomachines: from the basics to recent advances. *Advanced Functional Materials*, Vol. 28, No. 25, 2018, id. 1705872.

[99] Liu, J., J. Li, G. Wang, W. Yang, J. Yang, and Y. Liu. Bioinspired zeolitic imidazolate framework (ZIF-8) magnetic micromotors for highly efficient removal of organic pollutants from water. *Journal of Colloid and Interface Science*, Vol. 555, 2019, pp. 234–244.

[100] Yang, Z., L. Yang, M. Zhang, Q. Wang, S. C. H. Yu, and L. Zhang. Magnetic control of a steerable guidewire under ultrasound guidance using mobile electromagnets. *IEEE Robotics and Automation Letters*, Vol. 6, No. 2, 2021, pp. 1280–1287.

[101] Zhang, S., M. Yin, Z. Lai, C. Huang, C. Wang, W. Shang, et al. Design and characteristics of 3D magnetically steerable guidewire system for minimally invasive surgery. *IEEE Robotics and Automation Letters*, Vol. 7, No. 2, 2022, pp. 4040–4046.

[102] Zong, Z., X. Zhou, L. Zhang, Q. Tan, J. Xiong, and W. Zhang. Magnetically propelled soft micromachines with multipatterned fabrications. *Journal of Micromechanics and Microengineering*, Vol. 30, No. 8, 2020, id. 085001.

[103] Liao, P., L. Xing, S. Zhang, and D. Sun. Magnetically driven undulatory microswimmers integrating multiple rigid segments. *Small*, Vol. 15, No. 36, 2019, id. 1901197.

[104] Gu, H., Q. Boehler, H. Cui, E. Secchi, G. Savorana, C. De Marco, et al. Magnetic cilia carpets with programmable metachronal waves. *Nature Communications*, Vol. 11, No. 1, 2020, id. 2637.

[105] Sun, D., J. Zhang, Q. Fang, P. Xiang, Y. Xue, Y. Wang, et al. Analysis and control for a bioinspired multi-legged soft robot. *Biomimetic Intelligence and Robotics*, Vol. 2, No. 1, 2022, id. 100030.

[106] Mahalik, N. P. *Micromanufacturing and Nanotechnology*, Springer Berlin Heidelberg, 2006.

[107] Chen, C., S. Tang, H. Teymourian, E. Karshalev, F. Zhang, J. Li, et al. Chemical/Light-powered hybrid micromotors with “On-the-Fly” optical brakes. *Angewandte Chemie-International Edition in English*, Vol. 57, No. 27, 2018, pp. 8110–8114.

[108] Ji, S. C., X. Y. Li, Q. Y. Chen, P. Y. Lv, and H. L. Duan. Enhanced locomotion of shape morphing microrobots by surface coating. *Advanced Intelligent Systems*, Vol. 3, No. 7, 2021, id. 2000270.

[109] Ghosh, A., D. Dasgupta, M. Pal, K. I. Morozov, A. M. Leshansky, and A. Ghosh. Helical nanomachines as mobile viscometers. *Advanced Functional Materials*, Vol. 28, No. 25, 2018, id. 1705687.

[110] Pal, M., D. Dasgupta, N. Somalwar, V. R. Reshma, M. Tiwari, D. Teja, et al. Helical nanobots as mechanical probes of intra- and extracellular environments. *Journal of Physics: Condensed Matter*, Vol. 32, No. 22, 2020, id. 224001.

[111] Venkataramanababu, S., G. Nair, P. Deshpande, A. J. M. Mohan, S. Ghosh, and A. Chiro-plasmonic. Refractory metamaterial with titanium nitride (TiN) core-shell nanohelices. *Nanotechnology*, Vol. 29, No. 25, 2018, id. 255203.

[112] Venugopalan, P. L., S. Jain, S. Shivashankar, and A. Ghosh. Single coating of zinc ferrite renders magnetic nanomotors therapeutic and stable against agglomeration. *Nanoscale*, Vol. 10, No. 5, 2018, pp. 2327–2332.

[113] Kadiri, V. M., C. Bussi, A. W. Holle, K. Son, H. Kwon, G. Schutz, et al. Biocompatible magnetic micro- and nanodevices: Fabrication of FePt nanopropellers and cell transfection. *Advanced Materials*, Vol. 32, No. 25, 2020, id. e2001114.

[114] Huang, Z. J., G. C. P. Tsui, Y. Deng, and C. Y. Tang. Two-photon polymerization nanolithography technology for fabrication of stimulus-responsive micro/nano-structures for biomedical applications. *Nanotechnology Reviews*, Vol. 9, No. 1, 2020, pp. 1118–1136.

[115] Zheng, C. L., F. Jin, Y. Y. Zhao, M. L. Zheng, J. Liu, X. Z. Dong, et al. Light-driven micron-scale 3D hydrogel actuator produced by two-photon polymerization microfabrication. *Sensors and Actuators B: Chemical*, Vol. 304, 2020, id. 127345.

[116] Li, J., X. Li, T. Luo, R. Wang, C. Liu, S. Chen, et al. Development of a magnetic microrobot for carrying and delivering targeted cells. *Science Robotics*, Vol. 3, No. 19, 2018, id. eaat8829.

[117] Kim, E., S. Jeon, H. K. An, M. Kianpour, S. W. Yu, J. Y. Kim, et al. A magnetically actuated microrobot for targeted neural cell delivery and selective connection of neural networks. *Science Advances*, Vol. 6, No. 39, 2020, id. eabb5696.

[118] Wang, X., J. Cai, L. Sun, S. Zhang, D. Gong, X. Li, et al. Facile fabrication of magnetic microrobots based on spirulina templates for targeted delivery and synergistic chemo-photothermal therapy. *ACS Applied Materials & Interfaces*, Vol. 11, No. 5, 2019, pp. 4745–4756.

[119] Singh, A. V., M. H. D. Ansari, M. Mahajan, S. Srivastava, S. Kashyap, P. Dwivedi, et al. Sperm cell driven microrobots - emerging opportunities and challenges for biologically inspired robotic design. *Micromachines (Basel)*, Vol. 11, No. 4, 2020, id. 448.

[120] Gunputh, U. and H. Le. Biomedical composites. *Biomaterials Science*, 4th edn, Woodhead Publishing, London, 2017, pp. 59–82.

[121] Maeda, Y., T. Yasuda, K. Matsuzaki, Y. Okazaki, E. Pouget, R. Oda, et al. Common mechanism for helical nanotube formation by anodic polymerization and by cathodic deposition using helical pores on silicon electrodes. *Electrochemistry Communications*, Vol. 114, 2020, id. 106714.

[122] Naderi, L. and S. Shahrokhian. Nickel vanadium sulfide grown on nickel copper phosphide Dendrites/Cu fibers for fabrication of all-solid-state wire-type micro-supercapacitors. *Chemical Engineering Journal*, Vol. 392, 2020, id. 124880.

[123] Wang, Q., Y. Wang, B. Guo, S. Shao, Y. Yu, X. Zhu, et al. Novel heparin-loaded mesoporous tubular micromotors formed via template-assisted electrochemical deposition. *Journal of Materials Chemistry B: Materials for Biology and Medicine*, Vol. 7, No. 16, 2019, pp. 2688–2695.

[124] Chatzipirpiridis, G., C. de Marco, E. Pellicer, O. Ergeneman, J. Sort, B. J. Nelson, et al. Template-assisted electroforming of fully semi-hard-magnetic helical microactuators. *Advanced Engineering Materials*, Vol. 20, No. 9, 2018, id. 1800179.

[125] Chen, X. Z., M. Hoop, N. Shamsudhin, T. Huang, B. Ozkale, Q. Li, et al. Hybrid magnetoelectric nanowires for nanorobotic applications: Fabrication, magnetoelectric coupling, and magnetically assisted in vitro targeted drug delivery. *Advanced Materials*, Vol. 29, No. 8, 2017, id. 1605458.

[126] Jang, B., A. Hong, C. Alcantara, G. Chatzipirpiridis, X. Marti, E. Pellicer, et al. Programmable locomotion mechanisms of nanowires with semihard magnetic properties near a surface boundary. *ACS Applied Materials & Interfaces*, Vol. 11, No. 3, 2019, pp. 3214–3223.

[127] Ji, F., T. Li, S. Yu, Z. Wu, and L. Zhang. Propulsion gait analysis and fluidic trapping of swinging flexible nanomotors. *ACS Nano*, Vol. 15, No. 3, 2021, pp. 5118–5128.

[128] Li, T., J. Li, K. I. Morozov, Z. Wu, T. Xu, I. Rozen, et al. Highly efficient freestyle magnetic nanoswimmer. *Nano Letters*, Vol. 17, No. 8, 2017, pp. 5092–5098.

[129] Alcântara, C. C. J., S. Kim, S. Lee, B. Jang, P. Thakolkaran, J. Y. Kim, et al. 3D fabrication of fully iron magnetic microrobots. *Small*, Vol. 15, 2019, id. 1805006.

[130] Li, J., P. Angsantikul, W. Liu, B. Esteban-Fernandez de Avila, X. Chang, E. Sandraz, et al. Biomimetic platelet-camouflaged nanorobots for binding and isolation of biological threats. *Advanced Materials*, Vol. 30, No. 2, 2018, id. 1704800.

[131] Wang, H., X. Song, J. Xiong, and U. K. Cheang. Fabrication of bilayer magnetically actuated l-shaped microrobot based on chitosan via photolithography. *Polymers*, Vol. 14, No. 24, 2022, id. 5509.

[132] Huang, H.-W., F. E. Uslu, P. Katsamba, E. Lauga, M. S. Sakar, and B. J. Nelson. Adaptive locomotion of artificial microswimmers. *Science Advances*, Vol. 5, No. 1, 2019, id. eaau1532.

[133] Tan, L. and D. J. Cappelleri. Design, fabrication, and characterization of a helical adaptive multi-material microrobot (HAMMR). *IEEE Robotics and Automation Letters*, Vol. 8, No. 3, 2023, pp. 1723–1730.

[134] Yousefi, M. and H. Nejat Pishkenari. Independent position control of two identical magnetic microrobots in a plane using rotating permanent magnets. *Journal of Micro-Bio Robotics*, Vol. 17, No. 1, 2021, pp. 59–67.

[135] Gong, D., B. Li, N. Celi, J. Cai, and D. Zhang. Efficient removal of Pb (II) from aqueous systems using Spirulina-based biohybrid magnetic helical microrobots. *ACS Applied Materials & Interfaces*, Vol. 13, No. 44, 2021, pp. 53131–53142.

[136] Lee, S., J. Y. Kim, J. Kim, A. K. Hoshiar, J. Park, S. Lee, et al. A needle-type microrobot for targeted drug delivery by affixing to a microtissue. *Advanced Healthcare Materials*, Vol. 9, No. 7, 2020, id. e1901697.

[137] Schwarz, L., D. D. Karnaushenko, F. Hebenstreit, R. Naumann, O. G. Schmidt, and M. Medina-Sanchez. A rotating spiral micromotor for noninvasive zygote transfer. *Advanced Sciences (Weinh)*, Vol. 7, No. 18, 2020, id. 2000843.

[138] Lu, H., M. Zhang, Y. Yang, Q. Huang, T. Fukuda, Z. Wang, et al. A bioinspired multilegged soft millirobot that functions in both dry and wet conditions. *Nature Communications*, Vol. 9, No. 1, 2018, id. 3944.

[139] Lu, J., Y. Liu, W. Huang, K. Bi, Y. Zhu, and Q. Fan. Robust control strategy of gradient magnetic drive for microrobots based on extended state observer. *Cyborg and Bionic Systems*, Vol. 2022, 2022, id. 9835014.

[140] Fan, X., Y. Jiang, M. Li, Y. Zhang, C. Tian, L. Mao, et al. Scale-reconfigurable miniature ferrofluidic robots for negotiating sharply variable spaces. *Science Advances*, Vol. 8, No. 37, 2022, id. eabq1677.

[141] Xu, S., J. Liu, C. Yang, X. Wu, and T. Xu. A learning-based stable servo control strategy using broad learning system applied for microrobotic control. *IEEE Transactions on Cybernetics*, Vol. 52, No. 12, 2022, pp. 13727–13737.

[142] Liu, J., T. Xu, C. Huang, and X. Wu. Automatic manipulation of magnetically actuated helical microswimmers in static environments. *Micromachines*, Vol. 9, No. 10, 2018, id. 524.

[143] Xu, T., J. Liu, C. Huang, T. Sun, and X. Wu. Discrete-time optimal control of miniature helical swimmers in horizontal plane. *IEEE Transactions on Automation Science and Engineering*, Vol. 19, No. 3, 2022, pp. 2267–2277.

[144] Liu, J., T. Xu, and X. Wu. Model predictive control of magnetic helical swimmers in two-dimensional plane. *IEEE Transactions on Automation Science and Engineering*, 2023, pp. 1–10.

[145] Liu, J., X. Wu, C. Huang, L. Manamanchaiyaporn, W. Shang, X. Yan, et al. 3-D autonomous manipulation system of helical microswimmers with online compensation update. *IEEE Transactions on Automation Science and Engineering*, Vol. 18, No. 3, 2021, pp. 1380–1391.

[146] Xu, T., C. Huang, Z. Lai, and X. Wu. Independent control strategy of multiple magnetic flexible millirobots for position control and path following. *IEEE Transactions on Robotics*, Vol. 38, No. 5, 2022, pp. 2875–2887.

[147] Yang, L., J. Jiang, X. Gao, Q. Wang, Q. Dou, and L. Zhang. Autonomous environment-adaptive microrobot swarm navigation enabled by deep learning-based real-time distribution planning. *Nature Machine Intelligence*, Vol. 4, No. 5, 2022, pp. 480–493.

[148] Xu, H., M. Medina-Sanchez, M. F. Maitz, C. Werner, and O. G. Schmidt. Sperm micromotors for cargo delivery through flowing blood. *ACS Nano*, Vol. 14, No. 3, 2020, pp. 2982–2993.

[149] Iacovacci, V., L. Ricotti, E. Sinibaldi, G. Signore, F. Vistoli, and A. Menciassi. An Intravascular magnetic catheter enables the retrieval of nanoagents from the bloodstream. *Advanced Sciences (Weinh)*, Vol. 5, No. 9, 2018, id. 1800807.

[150] Wang, S., K. Liu, F. Wang, F. Peng, and Y. Tu. The application of micro- and nanomotors in classified drug delivery. *Chemistry – An Asian Journal*, Vol. 14, No. 14, 2019, pp. 2336–2347.

[151] Chen, W., Y. Wen, X. Fan, M. Sun, C. Tian, M. Yang, et al. Magnetically actuated intelligent hydrogel-based child-parent microrobots for targeted drug delivery. *Journal of Materials Chemistry B: Materials for Biology and Medicine*, Vol. 9, No. 4, 2021, pp. 1030–1039.

[152] Villa, K., L. Krejcova, F. Novotny, Z. Heger, Z. Sofer, and M. Pumera. Cooperative multifunctional self-propelled paramagnetic microrobots with chemical handles for cell manipulation and drug delivery. *Advanced Functional Materials*, Vol. 28, No. 43, 2018, id. 1804343.

[153] Lin, Z., X. Fan, M. Sun, C. Gao, Q. He, and H. Xie. Magnetically actuated peanut colloid motors for cell manipulation and patterning. *ACS Nano*, Vol. 12, No. 3, 2018, pp. 2539–2545.

[154] Go, G., S. G. Jeong, A. Yoo, J. Han, B. Kang, S. Kim, et al. Human adipose-derived mesenchymal stem cell-based medical microrobot system for knee cartilage regeneration in vivo. *Science Robotics*, Vol. 5, No. 38, 2020, id. eaay6626.

[155] Venugopalan, P. L., B. Esteban-Fernandez de Avila, M. Pal, A. Ghosh, and J. Wang. Fantastic voyage of nanomotors into the cell. *ACS Nano*, Vol. 14, No. 8, 2020, pp. 9423–9439.

[156] Wang, W., Z. Wu, and Q. He. Swimming nanorobots for opening a cell membrane mechanically. *View*, Vol. 1, No. 3, 2020, id. 20200005.

[157] Vyskocil, J., C. C. Mayorga-Martinez, E. Jablonska, F. Novotny, T. Ruml, and M. Pumera. Cancer cells microsurgery via asymmetric bent surface Au/Ag/Ni microrobotic scalpels through a transversal rotating magnetic field. *ACS Nano*, Vol. 14, No. 7, 2020, pp. 8247–8256.

[158] Xi, W., A. A. Solovev, A. N. Ananth, D. H. Gracias, S. Sanchez, and O. G. Schmidt. Rolled-up magnetic microdrillers: towards remotely controlled minimally invasive surgery. *Nanoscale*, Vol. 5, No. 4, 2013, pp. 1294–1297.

[159] Zhang, Y. B., K. Yuan, and L. Zhang. Micro/nanomachines: from functionalization to sensing and removal. *Advanced Materials Technology-Us*, Vol. 4, No. 4, 2019, id. 1800636.

[160] Xu, X., S. Hou, N. Wattanatorn, F. Wang, Q. Yang, C. Zhao, et al. Precision-guided nanospears for targeted and high-throughput intracellular gene delivery. *ACS Nano*, Vol. 12, No. 5, 2018, pp. 4503–4511.

[161] Wang, Z., Z. Xu, B. Zhu, Y. Zhang, J. Lin, Y. Wu, et al. Design, fabrication and application of magnetically actuated micro/nanorobots: a review. *Nanotechnology*, Vol. 33, No. 15, 2022, id. 152001.

[162] Jin, Q., Y. Yang, J. A. Jackson, C. Yoon, and D. H. Gracias. Untethered single cell grippers for active biopsy. *Nano Letters*, Vol. 20, No. 7, 2020, pp. 5383–5390.

[163] Dong, Y., L. Wang, K. Yuan, F. Ji, J. Gao, Z. Zhang, et al. Magnetic microswarm composed of porous nanocatalysts for targeted elimination of biofilm occlusion. *ACS Nano*, Vol. 15, No. 3, 2021, pp. 5056–5067.

[164] Mayorga-Martinez, C. C., J. Zelenka, K. Klima, P. Mayorga-Burrezo, L. Hoang, T. Ruml, et al. Swarming magnetic photoactive microrobots for dental implant biofilm eradication. *ACS Nano*, Vol. 16, No. 6, 2022, pp. 8694–8703.

[165] Sun, M., K. F. Chan, Z. Zhang, L. Wang, Q. Wang, S. Yang, et al. Magnetic microswarm and fluoroscopy-guided platform for biofilm eradication in biliary stents. *Advanced Materials*, Vol. 34, No. 34, 2022, id. e2201888.